Speciation and reaction equilibrium constant modelling of aqueous hydrometallurgical systems at elevated temperatures: A review

Okechukwu Vincent Dickson, Thomas Deleau, Christophe Coquelet, Fabienne Espitalier, Julien Lombart, Antoine Tardy, Fatima Lachaize

Chemical Thermodynamics and Thermal Analysis 11 (2023) 100117

Contents lists available at ScienceDirect

Chemical Thermodynamics and Thermal Analysis

journal homepage: www.elsevier.com/locate/ctta

Speciation and reaction equilibrium constant modelling of aqueous hydrometallurgical systems at elevated temperatures: A review

Okechukwu Vincent Dickson[a,c], Thomas Deleau[a], Christophe Coquelet[a,b,*], Fabienne Espitalier[a,b], Julien Lombart[c], Antoine Tardy[c], Fatima Lachaize[c]

[a] University of Toulouse, IMT Mines Albi, UMR CNRS 5302, RAPSODEE Centre, Campus Jarlard, Albi Cedex 09 F-81013, France
[b] Mines Paris, PSL University, CTP Centre Thermodynamique des Procédés, 35 rue Saint Honoré 77305 Fontainebleau Cedex, France
[c] Prony Resources New Caledonia, Usine du grand sud route de Kwa neie, Prony Bp 218, New Caledonia

ARTICLE INFO

Keywords:
Activity coefficient
Equilibrium constant
Hydrometallurgy
Speciation
Thermodynamics

ABSTRACT

Encrustation occurs in many processing fluids where high levels of dissolved solids are present, especially in processes that use heat transfer equipment. The deposition of these scales in the interior surfaces of an autoclave can cause major issues in the operation of industrial processes such as hydrometallurgy. The knowledge of the minerals' chemistry, distribution of the chemical forms of these minerals in the autoclave, and their solubility product can assist to inhibit these solid deposits. To model such systems, it is necessary to know the reactions involved and by extension their equilibrium constants. These electrolytic systems being strongly non-ideal, models of activity coefficients are necessary to deduce the concentration of each species. This review presents and compares various models for the calculation of activity coefficients and the thermodynamic equilibrium constants at temperatures above 25 °C. For model validity and comparison purposes, a case study on the speciation of the aqueous binary systems of H_2SO_4-$Al_2(SO_4)_3$ and H_2SO_4_$MgSO_4$ is presented and compared with experimental data. From the results obtained and in the framework presented above, the Density equilibrium constant model coupled with the Truesdell-Jones activity coefficient model gave the best fit with experimental data at the studied temperatures of 235, 250, 270, and 300 °C.

Introduction

High-pressure acid leaching (HPAL) is an excellent hydrometallurgical process for recovering nickel and cobalt from laterite ores due to its fast kinetics, stability of residues produced, and its selectivity against iron [1]. The process works at temperatures and pressures in the range of 230 - 270 °C [2] and 30 - 56 bar [3] respectively. Metals are separated based on their difference in solubilities and other electrochemical properties such as redox potentials and conductance of the metal [4]. The leaching mechanism in the autoclave involves the acid dissolution of the major constituent of the mineral matrix, followed by hydrolysis and precipitation of insoluble oxides and sulphates of iron, aluminium, and silica. The optimum leaching conditions vary according to the processed ore mineralogy [2], the particle size distribution, and the solid fraction [5,6]. A comprehensive study of the chemistry of elements involved in the pressure acid leaching of nickel laterite and parameters influencing the leaching system such as acid/ore ratio, ore grind (particle size), solid fraction, temperature, salts, and air addition has been studied by different authors and a summarised description is provided by Whittington & Muir [2] and Chou et al. [7].

The formation of complexes and the dissociation of electrolytes occur simultaneously in electrolytic solutions encountered during hydrometallurgical processing. The insoluble or slightly soluble complexes precipitate as a result of supersaturation leading to the formation of solids in suspension and scales at the autoclave wall. Aqueous electrolytic process modelling is gradually becoming a tool in the development, analysis, design, and control of hydrometallurgical processes [8]. In particular, chemical speciation defines the distribution of these species in different forms (i.e., solid or aqueous) in the autoclave.

Speciation calculations are performed for the determination of the chemical equilibrium composition in a system which provides information on the total amount of the species contained in that system. Direct speciation measurements (experimentally) are complex and require separate techniques [9,10]. Since most techniques are focused on the detection of free metal ion concentrations [11] or total metal concentrations [12], it is generally not possible to determine speciation analysis using only analytical chemistry methods. Although the capillary electrophoresis (CE) method allows the direct measurements of chemical speciation of some metals [13]. Since the environmental concentrations of most metals of interest are low and many relevant forms of metals cannot be measured directly, analytical techniques are often ineffective for the de-

* Corresponding author.
E-mail address: christophe.coquelet@mines-albi.fr (C. Coquelet).

https://doi.org/10.1016/j.ctta.2023.100117
Received 26 April 2023; Received in revised form 13 June 2023; Accepted 24 June 2023

Glossary of symbols

~	Used as a sign for dimensionless parameters
≈	Approximation sign
≡	Equivalence sign (the same as)
$\overline{Cp_j}^{\circ}$	The partial molal heat capacity of the aqueous species j at infinite dilution ($J.mol^{-1}K^{-1}$)
$\Delta G^{\circ}_{i,T}$	Change in standard Gibbs free energy of a reaction at a given temperature and pressure ($\frac{J}{mol}$)
$\Delta H^{\circ}_{i,T}$	Change in standard enthalpy of a species at a given temperature and pressure ($\frac{J}{mol}$)
$\Delta S^{\circ}_{i,T}$	Change in standard entropy of a reaction at a given temperature and pressure ($\frac{J}{mol.\ K}$)
ΔZ^2	The difference between the square of the charges of the reacting species (~)
A_γ	Debye-Hückel parameter ($kg^{\frac{1}{2}}\ mole^{-\frac{1}{2}}$)
B_γ	Debye-Hückel parameter ($kg^{\frac{1}{2}}\ mole^{-\frac{1}{2}}\ cm^{-1}$)
A_φ	Debye-Hückel osmotic coefficient ($kg^{\frac{1}{2}} mol^{-\frac{1}{2}}$)
B, B^0, B_1, B_2 and B_3, B_+, B_-	Parameters for ion interaction in Bromley's equation ($\frac{kg}{mol}$)
C^τ, β_0, β_1	Pitzer parameters specific to the ionic species (~)
Cp_{soln}	The heat capacity of a solution ($J.K^{-1}\ g^{-1}$)
$Cp^*_{H_2O}$	The molar heat capacity of water ($J{\cdot}K^{-1}mol^{-1}$)
Cp_ϕ	Apparent molal heat capacity ($J.mol^{-1}K^{-1}$)
K^0_T	The thermodynamic equilibrium constant at 25 °C and zero ionic strength (~)
K_{eq}	The thermodynamic equilibrium constant (~)
P°	Reference pressure (bar)
$S_{Cp} \equiv A_c\sqrt{\rho_w}$	Theoretical derivation of Debye-Hückel from the slope
a_j	The activity of a species (~)
b_b	Truesdell-Jones' parameter for activity coefficient calculation ($\frac{kg}{mol}$)
$c_{1,j} - c_{4,j}$, $a_{1,j} - a_{4,j}$	Temperature/pressure ionic specific independent HKF parameters (~)
m_j	The molality of a species ($\frac{mol}{kg}$)
$p_1 - p_9$, $q_1 - q_5$	Constant fitting parameters
v_+v_-	The stoichiometric coefficient for cation and anion respectively (~)
$\gamma^0_{25^oC}$	The experimental value reduced activity coefficient at 25 °C (~)
γ^0_T	The reduced activity coefficient at the desired temperature in the Meissner equation (~)
γ_i	The activity coefficient of a species (~)
$\delta_+\delta_-$	Bromley's parameters
ε_0, a, b	Parameters for Helgeson dielectric constant of water (~)
ε_T	The dielectric constant of H_2O (~)
μ_i	Reaction chemical potential for a given species ($\frac{J}{mol}$)
ω_j	The born coefficient for HKF parameter (~)
$\Delta C^{\circ}_{pj,T,P}$	Change in standard heat capacity of a reaction at a given temperature and pressure ($\frac{J}{mol.\ K}$)
e	Absolute electronic charge (4.80298 esu = 1.6021 × 10^{-9} Coulomb)
k	Boltzmann's constant (1.38065 × 10^{-16} erg.K $^{-1}$).
N	Avogadro's number (6.02252 × 10^{23} mol^{-1})
R	Ideal gas constant 8.3145 ($\frac{J}{K.mol}$)
T	Temperature (K or °C) - the unit used is specified in the equation
$\acute{\alpha}$	Ion size parameter which is also known as the "effective diameter of hydrated ion (Å)
I	Ionic strength (molal)
P	Pressure (bar)
X, Y, Z	The born function defined by Helgeson (K^{-1})
Z	The charge of ion species. Z_+ for cation, Z_- for anion (~)
$\exp \equiv e^i$	Exponential
ln	Natural logarithm
$\log \equiv \log_{10}$	logarithm in base 10
α	Pitzer constant. Also, the coefficient of thermal expansion of H_2O in Eq. (39) (~)
θ	Structural temperature (K)
π	pi = 3.14159265
ρ	Density of the medium in g/cm^3 (water = 0.9998 g/cm^3 at 25 °C and 1 bar)
ψ	Solvent-dependent parameter by Helgeson and Shock (2600 bar)

termination of the overall speciation [14]. Thus, the total distribution of species in a system is generally obtained from both analytical methods and chemical speciation models [14]. Aqueous speciation calculations use the chemical compositions of a system composed of liquid and solid as input and the distribution of species between the liquid and the solid phase as output [15]. These calculations need to take into account physicochemical processes such as complexation, hydrolysis, precipitation, dissolution, volatilization, oxidation, reduction, adsorption, and desorption [16]. This computation is based on the thermodynamic equilibrium constants of the dissociation/complexation reactions involved in the system and depends on the concentration of the different species in the system, the temperature, the pressure, and the activity coefficients of the chemical species in their molecular or electrolyte form. Three important points of this calculation are the knowledge of the reactions involved, the equilibrium constants of these reactions at the temperature of the system and the activity coefficients of the species involved in the reactions previously identified. For hydrometallurgy applications, identifying the reactions involved is a challenge given the plurality of elements present in the system (Co, Fe, Ni, Mg, Fe, Al, Mn, Cr, Si, S, e.t.c.). Moreover, since these reactions are carried out at temperatures higher

than the reference temperatures of the thermodynamic data, models are necessary to extrapolate the equilibrium constants to overcome the lack of experimental data. This review presents and compares different models classically used to obtain equilibrium constants and activity coefficients at higher temperature up to 300 °C. These models are compared and case studies presented to show the influence of model choice on the final result of a speciation calculation. In a first part, the bases of speciation calculation are presented. Then, the different models of calculation of equilibrium constants and activity coefficients are detailed and compared. Finally, the influence of the models and two case studies are presented. The models are described in details to allow the reproduction of the results presented. In addition, Matlab codes for the case studies are provided in the supplement.

Activity and activity coefficient of a species

Ionic compounds dissociate in a chemical system, resulting in the distribution of ions in the solution. These ions interact with each other and also with water molecules [17]. The interaction of these ions is considered, especially at higher ionic concentrations where these interactions are significant. The activity of a species is its effective concentration in a system and accounts for the non-ideal effects in aqueous systems, which include solvent-solvent, solvent-solute, and solute-solute interactions [18]. These effects are caused by the electrostatic forces between the ions dissolved in water [19].

The activity a_j

For a chemical species j, the activity a_j is defined as the product of its molality, m_j in mole per kilogram of solvent and its activity coefficient γ_j divided by m_j^o, the standard state molality, usually 1 mol.kg^{-1} for a solid and species in solution with infinite dilution:

$$a_j = \frac{\gamma_j \times m_j}{m_j^o} \tag{1}$$

For pure water and pure & crystalline solid species, $a_j = 1$ [1].

Activity coefficient γ_j

The activity coefficient γ_j of a species, j accounts for the deviation from an ideal mixing behaviour where the ions do not interact. It describes the intermolecular interaction between solutes and solvents [18,20]. Limited data on activity coefficients are available in the literature for ion species, especially at temperature, pressure, and ion concentrations of hydrometallurgical applications. Since the direct measurements of activity coefficient for high temperatures and pressure cannot be performed easily [21], a model exists for estimating them. Some of these empirical methods were resolved by Helgeson and Kirkham [22,23] and others [24–26]. The main models are presented below.

Debye- Hückel equation model

This theory provides a base point for most engineering models of electrolyte solutions. The limiting law which is a simplified version of the model valid for a very low ionic strength ($I < 10^{-3}$ molal) [27] is given as:

$$\log \gamma_j = -Z_j^2 A_\gamma \sqrt{I} \tag{2}$$

Taking into consideration the ion size parameter $\acute{\alpha}$ which is also known as the "effective diameter of hydrated ion", the extension of the Debye-Hückel equation for the activity coefficient of a dissociated binary electrolyte consisting of ions with charges can be written as:

$$\log \gamma_j = -\frac{Z_j^2 A_\gamma \sqrt{I}}{1 + \acute{\alpha} B_\gamma \sqrt{I}} \tag{3}$$

Z_j is the species charge, $\acute{\alpha}$ is the ion size parameter. The values of $\acute{a}$ for different species are reported by Kielland [28]. I is the ionic strength, which can be calculated using Eq. (4).

$$I = \frac{\sum m_j \times Z_j^2}{2} \tag{4}$$

In Eq. (3), the Debye-Hückel parameters A_γ and B_γ respectively can be computed from Eqs. (5) and (6) [23],

$$A_\gamma \equiv \frac{e^3 (2\pi N)^{\frac{1}{2}} \rho^{\frac{1}{2}}}{2.302585 (1000)^{\frac{1}{2}} (\varepsilon_T kT)^{\frac{3}{2}}} = \frac{1.824829238 \times 10^6 \rho^{\frac{1}{2}}}{(\varepsilon_T T)^{\frac{3}{2}}} \tag{5}$$

$$B_\gamma \equiv \sqrt{\frac{e^2 8\pi N \rho}{1000 \varepsilon_T kT}} = \frac{50.29158649 \times 10^8 \rho^{\frac{1}{2}}}{(\varepsilon_T T)^{\frac{1}{2}}} \tag{6}$$

where e is the absolute electronic charge, k the Boltzmann's constant, ρ the medium density and ε_T the dielectric constant of water at temperature. According to Helgeson, [29], the dielectric constant ε_T of water within the range of 0 - 370 °C can be determined from Eq. (7).

$$\varepsilon_{T,\ 1\ bar} = 305.7 \exp\left(-\exp(-12.741 + 0.0185T) - \frac{T}{219}\right) \tag{7}$$

T is the temperature in Kelvin.

The ion size parameter $\acute{\alpha}$ considers that ions are not point charges but rather have a finite radius. Values of $\acute{\alpha}$ for different ions in the extended Debye-Hückel equation are given in the literature [28]. The simplified Debye-Hückel equation is not suitable for solutions with ionic strength higher than 0.01 mol/kg. Experiments show that the results from the equation get worse as the ionic strength increases [30]. The extended Debye-Hückel equation expressed in Eq. (3) is more suitable and applicable for solutions with ionic strength $I \leq 0.1$ molal [27,31].

Truesdell-Jones (WATEQ Debye- Hückel) and Davies equation model

The Truesdell-Jones and Davies equations are a further extension of the Debye-Hückel theory to account for species with ionic strength greater than 0.1 mol/kg.

The Davies model presented in Eq. (8) is an extension of the Debye-Hückel giving a better fit to higher ionic strength. This equation is valid for ionic strengths up to 0.5 mol/kg.

$$\log \gamma_j = -Z_j^2 A_\gamma \left(\frac{\sqrt{I}}{1 + \sqrt{I}} - 0.3I\right) \tag{8}$$

In the Truesdell-Jones equation, an additional parameter is added to the Debye-Hückel equation which accounts for the observation that in high-ionic-strength experimental systems, the activity coefficients increase with increasing ionic strength. This model is applicable for ionic strength up to 2 mol/kg [32]. The Truesdell-Jones equation is expressed as:

$$\log \gamma_j = -\frac{Z_j^2 A_\gamma \sqrt{I}}{1 + \acute{\alpha} B_\gamma \sqrt{I}} + b_b I \tag{9}$$

where "b_b" and "$\acute{\alpha}$" are experimentally derived parameters. Note that even if $\acute{\alpha}$ has the same signification as in the Debye-Hückel equation, the values differ for each ionic species e.g. for H^+ $\acute{\alpha} = 0.9$ nm [28] in Eq. (3) and $\acute{a} = 0.478$ nm [33] in Eq. (9). The values of the parameters $\acute{a}$ and b_b in Eq. (9) for some species is given in the literature [32–34].

At ionic strengths between 0.001 and 0.0001 mol/kg, the separate curves for individual ions of the same valence converge on a single curve, the ions are very far apart in the solution and their interaction is accurately measured by their charge only. At these low ionic strengths, the term $\acute{\alpha} B_\gamma \sqrt{I}$ approaches zero, and the Debye-Hückel limiting equation is applied [32]. At higher ionic strengths greater than 0.01, differences in ion sizes become important and cause the γ_j curves for individual ions to diverge. Hence, the Extended Debye-Hückel's or Truesdell-Jones model is best suited for lower ionic strength in the range that the

Davies (0 - 0.6 mol/kg) model can compute because of the presence of the ion size parameter. As salt concentrations rise, ion size becomes significant, and the extended Debye- Hückel equation which includes a hydrated-ion size is needed to accurately model the activity coefficient values [32].

Bromley equation model

In strongly supersaturated solutions with high ionic strength up to 6 molal, the activity coefficient of aqueous electrolytes in the solution can be determined from Bromley's correlation as expressed in Eq. (10). Due to the exponential quality of the expression, extrapolation of the activity coefficient at higher ionic strength ($I > 6$ molal) introduces a great error [24,35].

$$\log \gamma_j = \frac{-|Z_+Z_-|\, A_\gamma \sqrt{I}}{1+\sqrt{I}} + \frac{(0.06+0.6B)|Z_+Z_-|I}{\left(1+\frac{1.5I}{|Z_+Z_-|}\right)^2} + BI \tag{10}$$

The values of A_γ are consistent with the Debye-Hückel constant. I is the ionic strength. $|Z_+Z_-|$ is the absolute value of the number of charges on the cation and/or anion. For example, $CaSO_4$ implies the charge of $Ca^{2+} = +2$ multiplied by the charge of $SO_4^{2-} = -2$, $|+2 \times -2| = 4$.

B (kg/mol) is the constant for ion interaction. The values of B for different salt species are reported by Bromley [24]. In the case where the salt is not listed, the value of 'B' is computed using the values tabulated by Bromley [24] depending on the type of salt with the equation.

$$B = B_+ + B_- + \delta_+\delta_- \tag{11}$$

For example, for $MgSO_4$;

$$B = B_{Mg^{2+}} + B_{SO_4^{2-}} + \left(\delta_{Mg^{2+}} \times \delta_{SO_4^{2-}}\right)$$

Bromley cautioned that the values are meant to be used for the calculation of the activity coefficients for only strong electrolytes that show complete dissociation. The major limitation of the Bromley equation is the fact that it does not consider the calculation of activity coefficient at higher temperatures since the tabulated B values are only available at 25 °C. Though he proposed two equations in which B is temperature dependent. The necessity for sufficient experimental data which is required to obtain the values of B^0, B_1, B_2 and B_3 is a major drawback to the equations.

$$B = B^0 \ln\left(\frac{T-243}{T}\right) + \frac{B_1}{T} + B_2 + B_3 lnT \tag{12}$$

$$B = \frac{B^0}{T-230} + \frac{B_1}{T} + B_2 + B_3 lnT \tag{13}$$

T (K) is the absolute temperature. Depending on the equation used, the four B constants are slightly different. Since the data for the parameter B are mostly not available, Bromley suggested the use of Meissner's method to determine the value at a given temperature if one good activity coefficient is known at a given ionic strength [24].

According to Meissner, at any ionic strength, the reduced activity can be found with Eq. (14) given the reduced activity coefficient at 25 °C is known [26]:

$$log(\gamma^0_{j,\,T}) = (1.125 - 0.005T)\log\left(\gamma^0_{25°C}\right) - (0.125 - 0.005T)\left(-\frac{0.41\sqrt{I}}{1+\sqrt{I}} + 0.039I^{0.92}\right) \tag{14}$$

I is the ionic strength, T (°C) is the temperature, γ^0_T is the reduced activity coefficient at the desired temperature, while $\gamma^0_{25°C}$ is the experimental value reduced activity coefficient at 25 °C at any ionic strength and can be obtained from the conversion to the mean molal activity coefficient obtained in Eq. (10) with the following expression $\gamma^0_{25°C} = \gamma^{\frac{1}{|Z_+Z_-|}}_{i(25°C)}$.

The mean molar activity coefficient $\gamma_{j(T)}$ at a given temperature can then be computed using Eq. (15) [26].

$$log(\gamma_j(T)) = |Z_+Z_-| log(\gamma^0_T) \tag{15}$$

Pitzer equation model

The Pitzer equation which is a more complex model derived from the modification of the Debye-Hückel, Guggenheim, Guntelberg, Davies, Bromley, and Meissner was modelled to account for solutions with higher ionic strength ≥ 6 molal [36]. It is the most complex model amongst the 4 stated models [27,37]. The model is a virial equation in concentration that yields the osmotic pressure [27,30].

$$ln(\gamma_j) = -A_p|z_+z_-| + B_p\left(\frac{2v_+v_-}{v_T}\right)m + C_p\left(\frac{2(v_+v_-)^{\frac{3}{2}}}{v_T}\right)m^2 \tag{16}$$

where

$$A_p = A_\varphi\left(\frac{\sqrt{I}}{1+1.2\sqrt{I}} + \frac{2}{1.2}\ln\left(1+1.2\sqrt{I}\right)\right) \tag{17}$$

$$A_\varphi = \frac{1}{3}\left(\frac{2\pi N\rho}{1000}\right)^{\frac{1}{2}}\left(\frac{e^2}{\varepsilon_T kT}\right)^{\frac{3}{2}} \tag{18}$$

The Debye-Hückel osmotic coefficient A_φ has the dimension of $(kg^{1/2}mol^{-1/2})$. The values of ε_T, k, e, N, and ρ are defined in Eqs. (5) and (6). $A_\varphi = 0.3915$ at 25 °C [25].

v_+v_- is the stoichiometric coefficient for the cation and the anion. $|z_+z_-|$ is the charges on the species of the compounds, e.g., for $AlCl_3$, $v_+v_- = 1 \times 3$, $v_T = 1+3$, $|z_+z_-| = |+3 \times -1|$. For Na_2SO_4, $v_+v_- = 2 \times 1$, $v_T = 1+2$ $|z_+z_-| = |+1 \times -2|$.

$$B_p = 2\beta_0 + \frac{2\beta_1}{\alpha^2 I}\left(1 - \left(1+\alpha\sqrt{I} - 0.5\alpha^2 I\right)\exp\left(-\alpha\sqrt{I}\right)\right) \tag{19}$$

$$C_p = \frac{3}{2}C^\tau \tag{20}$$

I is the ionic strength, constant $\alpha = 2$ with the dimension $[I]^{-\frac{1}{2}}$, m = concentration of the solution in molality (mol/kg), β_0, β_1 and C^τ are the Pitzer parameters specific to the ionic species, their values for different acids, bases, and salt complexes of 1–1 type, 2–1 type, 3–1 type, and 2–2 type can be seen in the report of Pitzer [25].

The difficulty in Pitzer equations for predicting activity coefficients in a system lies in the insufficient data for the large number of interaction parameters that have to be considered.

Equilibrium constant computation

The equilibrium constant is a state at which the value of a reaction quotient when none of its properties changes with time, irrespective of the duration, and would return to that state after being disturbed (chemical equilibrium). Thermodynamically speaking, a system is at equilibrium when the change in Gibbs free energy is equal to zero [31]. The speciation of a chemical system along with other parameters depends on the value of the equilibrium constant to predict the solubility and saturation index of a given system. The equilibrium constant helps us to know the concentrations of the species involved in a reaction and the extent of the reaction depicting where the equilibrium lies in a system, either favouring the reactant or the product.

Chemical equilibrium constant

The equilibrium constant of a given chemical reaction is the value of its reaction quotient at chemical equilibrium. It is affected by reaction parameters such as temperature, solvent, and ionic strength. Knowledge of the equilibrium constant is essential to understanding many chemical systems. Unlike a change in pressure or concentration of the reactants, temperature changes result in changes in the value of the equilibrium constant. For an exothermic reaction, an increase in temperature leads to a decrease in the value of the equilibrium constant, and vice versa for an endothermic reaction. When the equilibrium constant's value is very high, the concentration of the products will be much higher than

the concentration of the reactants. This means that the product predominates. A small value implies that the reactants are predominant at equilibrium.

The equilibrium constant can be in the form of stability (binding, formation) constants, association constants, and dissociation constants. The stability constant is a type of equilibrium constant for complex formations in a solution. It measures the strength of the interaction between the reagents that come together to form complexes and provides the information required to calculate the concentrations of the complexes in a solution. The dissociation constant, on the other hand, measures the tendency of a larger object to reversibly break down into smaller components, as seen when a complex breaks down into its molecular constituents, or when a salt splits up into its constituent ions.

Consider a reaction with the following expression in Eq. (21),

$$\nu_A A + \nu_B B \Leftrightarrow \nu_C C + \nu_D D \tag{21}$$

Where ν_A, ν_B, ν_C and ν_D are the stoichiometry coefficients of the reactants (A, B) and the products (C, D) respectively.

The chemical potential of the species for each reaction component in Eq. (21) is given as:

$$\mu_A(T,\ P) = \mu_A^0 + RT\ \ln a_A$$

$$\mu_B(T,\ P) = \mu_B^0 + RT \ln a_B$$

$$\mu_C(T,\ P) = \mu_C^0 + RT \ln a_C$$

$$\mu_D(T,\ P) = \mu_D^0 + RT \ln a_D$$

The reaction rate of μ which is the difference between the products and reactants is expressed as:

$$\Delta_r\mu_i(T,\ P) = \nu_D\mu_D + \nu_C\mu_C - \nu_A\mu_A - \nu_B\mu_B$$

$$\Delta_r\mu_i(T,\ P) = \nu_D\left(\mu_D^0 + RT\ln a_D\right) + \nu_C\left(\mu_C^0 + RT \ln a_C\right) - \nu_A\left(\mu_A^0 + RT \ln a_A\right) - \nu_B\left(\mu_B^0 + RT \ln a_B\right)$$

$$\Delta_r\mu_i(T,\ P) = \left(\nu_D\mu_D^0 + \nu_C\mu_C^0 - \nu_A\mu_A^0 - \nu_B\mu_B^0\right) + RT \ln a_D^{\nu_D} + RT \ln a_C^{\nu_C} - RT \ln a_A^{\nu_A} - RT \ln a_B^{\nu_B}$$

The chemical potential reaction rate of Eq. (21) is given as:

$$\Delta_r\mu_i(T,\ P) = \Delta_r\mu_i^o + RT\ ln\left(\frac{a_D^{\nu_D}.a_C^{\nu_C}}{a_A^{\nu_A}.a_B^{\nu_B}}\right) \tag{22}$$

And, Eq. (22) is generally expressed as:

$$\Delta_r\mu_i(T,\ P) = \Delta_r\mu_i^o + RT\ ln\prod_i a_i^{\upsilon_i} \tag{23}$$

When a reaction in a given system attains an equilibrium state, $\Delta_r\mu_i(T, P)$ becomes zero. The mathematical operator symbol ($\prod$) in Eq. (23) is then referred to as the equilibrium constant which is dependent on temperature and/or pressure. Thus, the equilibrium constant for a reaction i is expressed as:

$$K_{(i)}(T,\ P) = \prod_i a_i^{\upsilon_i} \tag{24}$$

where ν_i is the stoichiometric coefficient of the reaction species. At thermodynamic equilibrium, the chemical potential reaction rate equates to zero [38] and Eq. (23) and (24) gives:

$$\Delta_r\mu_i^o(T, P) = -RTlnK_{i,\ T,\ P} \tag{25}$$

For aqueous standards, the term $\Delta\mu_i^\circ = \Delta G_i^\circ$, where G_i° is the Gibbs free energy of the reaction.

$$\Delta_r\mu_i^o(T) \equiv \Delta G_{i,T}^\circ = \Delta H_{i,T}^\circ - T\Delta S_{i,T}^\circ = -RT\ ln\ K_{i,T} \tag{26}$$

The change in standard enthalpy of the reaction $\Delta H_i^\circ(T)$, change in standard entropy $\Delta S_i^\circ(T)$ and change in the standard heat capacities $\Delta C_{pi}^\circ(T)$ of any species 'j' in a reaction 'i', can be determined by Hess laws as shown in Eqs. (27) - (29).

$$\Delta H_{i,T}^\circ = \sum_j^{products} \nu_{i,j}\ \overline{H}_j^\circ(T) - \sum_j^{reactants} \nu_{i,j}\ \overline{H}_{j,T}^\circ \tag{27}$$

$$\Delta S_{i,T}^\circ = \sum_j^{products} \nu_{i,j}\ \overline{s}_{j,T}^\circ - \sum_j^{reactants} \nu_{i,j}\ \overline{s}_{j,T}^\circ \tag{28}$$

$$\Delta C_{pi,T}^\circ = \sum_j^{products} \nu_{i,j}\ C_{pj,T}^\circ - \sum_j^{reactants} \nu_{i,j}\ C_{pj,\ T}^\circ \tag{29}$$

The standard Gibbs free enthalpy can also be written as a sum of partial standard Gibbs free enthalpies:

$$\Delta G_{i,T}^\circ = \sum_j \nu_{i,j}\ \Delta\overline{G}_{j,T}^\circ \tag{30}$$

The value for $K_{i,\ T}$ is temperature-dependent. At higher temperatures, $K_{i,\ T}$ increases favouring forward reaction for an endothermic reaction while it decreases at a lower temperature, favouring backward reaction for an exothermic reaction.

Extrapolation of the equilibrium constant to elevated temperature

The thermodynamic equilibrium constant at 298.15 K and P° = 1 atm is convenient to obtain with Eq. (26) provided the values for the standard thermodynamic properties are available. But the determination of thermodynamic equilibrium constant at higher temperatures is challenging. The accuracy of the obtained equilibrium constant value will strongly depend on the accuracy of the thermodynamic data and the model used for the extrapolation. The various methods that can be used for high-temperature extrapolation of the equilibrium constant are reviewed below.

Determination of the equilibrium constant from the Gibbs standard free energy

For a reaction species in which the standard Gibbs free energy and the standard entropy are known at the reference state i.e. 298.15 K, and the value of the standard heat capacity known at a specified temperature, the standard Gibbs free energy of the reaction at that given temperature can be obtained from Eq. (31) [39].

$$\Delta G_{i,T}^\circ = \Delta G_{i,298.15}^\circ - \Delta s_{i,298.15}^\circ\ (T - 298.15) - T\int_{298.15}^{T}\frac{\Delta C_{pi,T}^\circ}{T}dT + \int_{298.15}^{T}\Delta C_{pi,T}^\circ dT \tag{31}$$

where T (K) is the temperature. The value of $C_{pj,T}^\circ$ for a species can be determined at a given temperature if the experimental data for A_1, B_1 and C_1 values are known using the Maier-Kelley correlation [40].

$$C_{pj,T}^\circ = A_1 + B_1\ T + C_1\ T^{-2} \tag{32}$$

However, the heat capacity values for some species that are involved in the equilibrium reactions are not usually available, and, in a few cases, their availability is at 25 °C. In such cases, the calculation of temperature-dependent thermodynamic properties for aqueous ions is done by extrapolation.

Determination of the equilibrium constant at higher temperatures by direct computation

The equilibrium constant of a reaction can be obtained without the computation of the standard Gibbs free energy at a given temperature. This means the values are extrapolated directly at the desired temperature without the utilization of Eq. (26) as far as the necessary thermodynamic data and associated parameters are available.

Neglection of the variation of specific heat capacity $\Delta C^{\circ}_{pi,T} = 0$

The van't Hoff's equation [41] expressed in Eq. (33) assumes that the specific heat capacity of a reaction is zero. The assumption that takes $\Delta C^{\circ}_{pi,T} = 0$ is too strong for the dissociation of most complexes and leads to errors when it is used to determine the value of log K_i(T) at higher temperatures [29].

$$ln\left(K_{i,\,T}\right) = ln\left(K_{i,298.15}\right) - \frac{\Delta H^{\circ}_{i,298.15}}{R}\left(\frac{1}{T} - \frac{1}{298.15}\right) \tag{33}$$

Neglection of the variation of heat capacities with temperature $\Delta C^{\circ}_{pi,T} = Cst$

If heat capacity data are available in the literature at the reference state, it is preferable not to neglect the variation of heat capacities, but only its variation with temperature. Assuming constant heat capacity $\Delta C^{\circ}_{pi,T} = \Delta C^{\circ}_{pi,298.15\ K}$, the equilibrium constant can be determined with the expression in Eq. (34) [42].

$$ln\left(K_{i,\,T}\right) = ln\left(K_{i,298.15}\right) - \frac{\Delta H^{\circ}_{i,298.15}}{R}\left(\frac{1}{T} - \frac{1}{298.15}\right) + \frac{\Delta C^{\circ}_{pi,298.15}}{R}\left(ln\left(\frac{T}{298.15}\right) + 298.15\left(\frac{1}{T} - \frac{1}{298.15}\right)\right) \tag{34}$$

The utilisation of the density model

The Density model is based on the heat capacity variation of a reaction which uses reference state values and the solvent properties, especially the temperature derivative of the thermal expansion coefficient of water [43]. This is a simple model that allows the estimation of several thermodynamic parameters for aqueous reactions at elevated temperatures and pressures [38]. The model gives the same accuracy as the revised Helgeson-Kirkham-Flowers (HKF) model as indicated in the literature, provided the available low-temperature thermodynamic data are reliable [43,44]. For reactions involving only aqueous species, the correlation in Eq. (35) is used.

$$ln\left(K_{i,\,T}\right) = ln\left(K_{i,298.15}\right) - \frac{\Delta H^{\circ}_{i,298.15}}{R}\left(\frac{1}{T} - \frac{1}{298.15}\right) + \frac{\Delta C^{\circ}_{pi,298.15}}{298.15R\left(\frac{\partial \alpha}{\partial T}\right)_{P^{\circ}=1\ bar}} \times \left(\frac{1}{T} ln\left(\frac{\rho_{(298.15\ K,\ 1bar)}}{\rho(T,P)}\right) - \frac{\alpha_{298.15}}{T}(T - 298.15)\right) \tag{35}$$

where α is the coefficient of thermal expansion of H_2O whose values are documented by Anderson [43] for pressure and temperature up to 10 kbar and 1000 °C respectively. ρ is the density of water at a given temperature. The thermodynamic properties of pure water at specific temperatures can be obtained from thermodynamic models [45]. The values for the density of the medium at a defined temperature and pressure ρ(T, P) have been estimated by Anderson et al., [43] at temperatures 25 - 1000 °C and pressures up to 10 kbar. To use this equation, the data for $K_{i,298.15}$, $\Delta H^{\circ}_{i,298.15}$, $\Delta C^{\circ}_{pi,298.15}$ as well as the density ρ over a temperature range close to that in which one wishes to operate is needed.

The density of water as a function of temperature and pressure can be computed using the correlation by Batzle & Wang [46] in Eq. (36) for temperature and pressure up to 573.15 K and 200 MPa respectively.

$$\rho(T,P) = 1 + 10^{-6} \times \left(-80T - 3.3T^2 + 0.00175T^3 + 489P - 2(T \times P) + 0.016T^2P - 1.3 \times 10^{-5}(T^3 \times P) - 0.333P^2 - 0.002T \times P^2\right) \tag{36}$$

where ρ(T, P) is the temperature and pressure-dependent density (g/cm^3), P is the pressure in MPa, and T is the temperature in (°C). In instances where the influence of pressure is not considered, the density of water can also be determined with an empirical equation as a function of temperature devised by Tödheide [47] as expressed in Eq. (37) for up to 1000 °C.

$$\rho(T) = 15.81747 + 9.87802T - 0.035239T^2 + \left(5.38051 \times 10^{-5}\right)T^3 - \left(3.2612 \times 10^{-8}\right)T^4 \tag{37}$$

where ρ(T) is the temperature-dependent density (kg/m^3) and T in (K).

The specific heat capacities are known as a function of temperature

In the case where the heat capacities are known at the desired temperature to be extrapolated. The equilibrium constant of a reaction at a given temperature can be calculated from Eq. (38):

$$ln\left(K_{i,\,T}\right) = ln\left(K_{i,298.15}\right) - \frac{\Delta H^{\circ}_{i,298.15}}{R}\left(\frac{1}{T} - \frac{1}{298.15}\right) + \frac{\Delta a_i}{R}\left(ln\frac{T}{298.15} + \frac{298.15}{T} - 1\right) + \frac{\Delta b_i}{2R}\left(T + \frac{298.15^2}{T} - 2 \times 298.15\right) + \frac{\Delta c_i}{R}\left(\frac{-T^2 - 298.15^2 + 2T \times 298.15}{2 \times 298.15^2 T^2}\right) + \frac{\Delta C^{\circ}_{pi,298.15}}{298.15R\left(\frac{\partial \alpha}{\partial T}\right)_{P^{\circ}=1\ bar}} \times \left(\frac{1}{T} ln\left(\frac{\rho_{(298.15K,\ 1bar)}}{\rho(T,P)}\right) - \frac{\alpha_{298.15}}{T}(T - 298.15)\right) \tag{38}$$

This equation is used for reactions involving both minerals and aqueous species [43], where a_i, b_i, c_i are the coefficient of Maier-Kelley heat capacities for a component. $\Delta a_i = \sum_j a_{i,j}$, $\Delta b_i = \sum_j b_{i,j}$, $\Delta c_i = \sum_j c_{i,j}$.

The ratio of heat capacity change at temperature is constant

With the assumption that $\Delta C^{\circ}_{pi,298.15}$ is proportional to $\Delta C^{\circ}_{pi,T}$, Helgeson [29,48] suggested that log($K_{i,\,T}$) can be computed directly using the expression in Eq. (39).

$$log\left(K_{i,\,T}\right) = \frac{\Delta S^{\circ}_{i,298.15}}{2.303RT}\left(298.15 - \frac{\theta}{w}\left(1 - exp\left(exp(b + aT) - c + \frac{T - 298.15}{\theta}\right)\right)\right) - \frac{\Delta H^{\circ}_{i,298.15}}{2.303RT} \tag{39}$$

where $\theta = 219$, $a = 0.01875$, $b = -12.741$, $c = 0.000784$, $w = 1.003229$

This equation assumes that the ratio of the heat capacity change at the reference temperature to the heat capacity change at T is constant ($\Delta C^{\circ}_{pi,298.15} / \Delta C^{\circ}_{pi,T}$ = cst). The assumption is more accurate for temperatures up to 423.15 - 473.15 K. Above this limit, the influence of electrostatic contribution becomes strong as the dielectric constant of water decreases with increasing temperature and the equation does not hold for higher temperatures [29].

The equation is applied only where the enthalpy and entropy of dissociation at 298.15 K are both negative. This is also true for certain reactions for which $\Delta H^{\circ}_{i,T}$ is a large positive number and $\Delta S^{\circ}_{i,T}$ is a negative number, an example of which is the dissociation of water reaction [29]. The equation is not applicable when the heat capacity of dissociation and/or $\Delta H^{\circ}_{i,298.15\ K}$ and $\Delta S^{\circ}_{i,298.15\ K}$ are both positive. Furthermore, the equation is not relevant when $\Delta H^{\circ}_{i,298.15}$ is a largely negative number and the $\Delta S^{\circ}_{i,298.15}$ is a positive number [29]. This equation gives a similar result to the equilibrium constant value computed from Eq. (41) provided the constraints of Eq. (39) are obeyed.

From the several approximation methods developed for the calculation of log($K_{i,\,T}$) where little or no heat capacity data are available, the assumption ($\Delta C^{\circ}_{pi,298.15} / \Delta C^{\circ}_{pi,T}$ = constant) is conceivably the most practical and accurate method than those based on the assumption that $\Delta C^{\circ}_{pi,T}$ = constant [29].

Determination from regressed experimental data correlation

In the case that the values of $\Delta H^{\circ}_{i,T}$, $\Delta s^{\circ}_{i,T}$ and $\Delta C^{\circ}_{p\,i,T}$ are not known. From regressed experimental data in the literature, as presented in the "Thermoddem database" [49] information on some aqueous species and solids can be gotten. The correlation stated in Eq. (40) gives the value of log($K_{i,\,T}$) at the desired temperature and the obtained result is best suited for most aqueous species than the values determined with van't Hoff's and other equations that do not consider the effect of heat capacity.

$$log\left(K_{i,\,T}\right) = A + BT + CT^{-1} + Dlog(T) + ET^{-2} \tag{40}$$

T (K) is the desired temperature the value for log($K_{i,\,T}$) is to be obtained, while A, B, C, D, and E are parameters determined experimentally.

The use of the unexpanded Helgeson model

If experimental heat capacity data is not known, extrapolation with the unexpanded Helgeson model can be used to determine the value of the standard free energy change [29,39] with the correlation in Eq. (41).

$$\Delta G^{\circ}_{i,\,T} = -\Delta S^{\circ}_{i,298.15}\left(298.15-\theta_1\left(1-exp\left(exp(\theta_2+\theta_3 T)+\theta_4+\frac{T-298.15}{\theta_5}\right)\right)\right) + \Delta H^{\circ}_{i,298.15} \quad (41)$$

where $\theta_1 = 218.3$ K, $\theta_2 = -12.741$, $\theta_3 = 0.01875\ K^{-1}$, $\theta_4 = -7.84 \times 10^{-4}$ and $\theta_5 = 219$ K If the data for $\Delta S^{\circ}_{i,298.15}$ are not present in the literature, a correlation for oxygenated molecules of the type XO_n^{-Z} has been developed [50].

$$\Delta S^{\circ}_{i,\,298.15} = 182 - 195(z - 0.28n) \quad (42)$$

z is the absolute value of the ion charge and n is the number of oxygen atoms. For acid oxy-anions, the number of OH^--group is subtracted from n [39].

When $\Delta G^{\circ}_{i,T}$ at a given temperature is computed, the correlation in Eq. (26) can be used to determine the value of the equilibrium constant at that temperature.

The use of the revised Helgeson model (HKF)

The revised Helgeson-Kirkham-Flowers (HKF) model with multiple parameters as shown in Eq. (43) is used in the calculation of the standard Gibbs free energy of any aqueous species at high temperature and pressure [40]. The equation considers the dielectric constant of water, the species-dependent equation-of-state parameters, and the solvent-dependent parameters at a given temperature as well as the pressure-independent parameters for aqueous species. Due to the complexity of the equation and its demand for many parameters, the practical application of this model requires its incorporation into some software such as SUPCRT92, and OLI-Systems® [1] for the calculation of thermodynamic equilibria at elevated temperatures and pressures.

$$\begin{aligned}\Delta G^{\circ}_{i,T} = {} & \Delta G^{\circ}_{i,298.15} - \Delta S^{\circ}_{i,298.15}(T-298.15) - c_1\left[T\ln\left(\frac{T}{298.15}\right) - T - 298.15\right] \\ & + a_1(P-P^{\circ}) + a_2\ln\left(\frac{\psi+P}{\psi+P^{\circ}}\right) + \left[a_3(P-P^{\circ}) + a_4\ln\left(\frac{\psi+P}{\psi+P^{\circ}}\right)\right]\left(\frac{1}{T-\theta}\right) \\ & - c_2\left[\left(\left(\frac{1}{T-\theta}\right) - \left(\frac{1}{298.15-\theta}\right)\right)\left(\frac{\theta-T}{\theta}\right) - \frac{T}{\theta^2}\ln\left(\frac{298.15(T-\theta)}{T(298.15-\theta)}\right)\right] \\ & + \omega\left(\frac{1}{\varepsilon_T}-1\right) + \omega_{P^{\circ},298.15}\left(\frac{1}{\varepsilon_{P^{\circ},298.15}}-1\right) + \omega_{P^{\circ},298.15}Y_{P^{\circ},298.15}(T-298.15)\end{aligned} \quad (43)$$

where T (K) is the desired temperature for extrapolation, P and P° are the desired pressure and the reference pressure (1 bar). a_1, a_2, a_3, a_4 are pressure-independent parameters. c_1, c_2 are independent parameters of the aqueous species' temperature. Y is the Born function, defined by $Y = \frac{1}{\varepsilon_T}\left(\frac{\partial \ln(\varepsilon_T)}{\partial T}\right)_P$. In the standard reference state $Y_{P^{\circ},298.15\ K} = -5.8 \times 10^{-5}\ K^{-1}$, [51]. θ and ψ are parameters dependent on the solvent (θ = 228 K and ψ = 2600 bar for water). ω is the equation of the state parameter on which the species depends while ε_T is the temperature-dependent dielectric constant of the medium (e.g., water).

The values for these parameters are essential when the HKF model is to be used in calculations and the values of some of these parameters for some species are documented in the reports of Shock and Helgeson [40,52].

Determination of heat capacity from apparent molal heat capacity of aqueous electrolyte

Heat capacity has a great influence on equilibrium constant computation and cannot be neglected especially in cases where the value of $\Delta H^{\circ}_{i,298.15}$ is small such as dissociation reactions [29]. According to statistical thermodynamics, heat capacity depends on the vibrational frequency of the atoms around their equilibrium positions. The higher the frequency, the lower the probability of heat absorption [53]. It can be determined by numerous experimental measurements in the laboratory of which the determination by differential scanning calorimetric or flow calorimetric techniques is common with great accuracy. The values can equally be calculated from the results of experiments that give the enthalpy data as a function of temperature for a given process [54]. Considering the importance of heat capacity in the determination of the equilibrium constant of aqueous species in chemical processes, it is paramount to obtain the Cp value given that the models that incorporate the effect of heat capacity yield precise results.

From the result of calorimetric measurement, the determination of the partial molal heat capacity of aqueous electrolytes and some related undissociated species can be expressed in terms of apparent molal heat capacities [21,55] as:

$$Cp_{\phi} = \frac{Cp_{soln} - n_1 Cp^{*}_{H_2O}}{n_2} \quad (44)$$

where, Cp_{soln} is the heat capacity of a solution containing n_1 moles of water and n_2 moles of solute. $Cp^{*}_{H_2O}$ is the molar heat capacity of water ($J{\cdot}K^{-1}{\cdot}mol^{-1}$).

For binary system (solute + solvent), the apparent molal heat capacity $Cp_{\phi}(JK^{-1}mol^{-1})$ of the aqueous solution can be computed from measured specific heat with the expression in Eq. (45) [56–60].

$$Cp_{\phi} = M.Cp^{exp}_{soln} + \left[\frac{1000\left(Cp^{exp}_{soln} - Cp^{o}_{H_2O}\right)}{m}\right] \quad (45)$$

Cp^{exp}_{soln} is the experimental value ($J.K^{-1}\,g^{-1}$) for the specific heat capacity of the solution, M is the molar mass ($\frac{g}{mol}$) of the electrolyte (solute), m is the molality ($\frac{mol}{kg}$) and $Cp^{o}_{H_2O}$ is the specific heat capacity of pure water 4.182 $J.K^{-1}\,g^{-1}$ at 25 °C. At infinite dilution (molality = 0), $Cp_{\phi} = \overline{Cp_j}^{\circ}$.

Theoretical determination of heat capacity

The theoretical determination of heat capacities has been reported by different authors [25,37,61], and different correlations developed for its computation by considering the partial and/or apparent molal quantities.

Pitzer ion interaction equation

The modelling of apparent molal heat capacity Cp_{ϕ} for any salt type in aqueous solutions at a high concentration can be done with the Pitzer model [25,54,62]. For a more concentrated electrolyte solution, the complex Pitzer virial coefficient equation in Eq. (46) is very suitable for the determination of the Cp_{ϕ} values [56].

$$\begin{aligned}Cp_{\phi} = {} & \overline{Cp_j}^{\circ} + (\upsilon_+ + \upsilon_-)|z_+ z_-|\left(\frac{A_j}{2.4}\right)\ln\left(1+1.2\sqrt{I}\right) \\ & - 2\upsilon_+\upsilon_- RT^2\left[mB^j_{\pm} + m^2\left(\upsilon_+ z_+\right)C^j_{\pm}\right]\end{aligned} \quad (46)$$

$$B^{j}_{\pm} = \left(\frac{\partial^2 B_{\pm}}{\partial T^2}\right)_{p,\,I} + \frac{2}{T}\left(\frac{\partial B_{\pm}}{\partial T}\right)_{p,\,I} \equiv \beta^{(0)j} + 2\beta^{(1)j}\left(\frac{1-\left(1+\alpha\sqrt{I}\right)\exp\left(-\alpha\sqrt{I}\right)}{\alpha^2 I}\right) + 2\beta^{(2)j}\left(\frac{1-\left(1+\alpha_2\sqrt{I}\right)\exp\left(-\alpha_2\sqrt{I}\right)}{\alpha_2^2 I}\right)$$

$$C^{j}_{\pm} = \left(\frac{\partial^2 C_{\pm}}{\partial T^2}\right)_p + \frac{2}{T}\left(\frac{\partial C_{\pm}}{\partial T}\right)_p \equiv C^{(0)j} + 4C^{(1)j}\frac{\left(6-\left(6+6\alpha_3\sqrt{I}+3\alpha_3^2 I+\alpha_3^3 I^{\frac{3}{2}}\right)\exp\left(-\alpha_3\sqrt{I}\right)\right)}{\alpha_3^4 I^2}$$

$\overline{Cp}^{\circ}_{j}$ is the partial molal heat capacity of the aqueous species j at infinite dilution with respect to temperature and pressure [61]. v_+v_- are the stoichiometric coefficient for the cations and anions in an electrolyte and z_+z_- are their respective ionic charges. The parameter $C^{j}_{\pm}$ is independent of ionic strength while $B^{j}_{\pm}$ depends on ionic strength [54]. I and m are the ionic strength and molality respectively. $\alpha = 2.0$ $kg^{1/2}mol^{-1/2}$ for other electrolyte salt types (1–1 type e.g. NaCl, 2–1 type e.g. $MgCl_2$, etc.) except for 2–2 types such as $MgSO_4$, $NiSO_4$, $CoSO_4$, and $MnSO_4$ with $\alpha = 1.4$ as a result of their electrostatic ion pairing effect with solvent, $\alpha_2 = 12$ $kg^{1/2}mol^{-1/2}$ [25]. α_3 was modelled to be 1 $kg^{1/2}mol^{-1/2}$ by Archer & Rard [63]. $\beta^{(0)j}$, $\beta^{(1)j}$, $\beta^{(2)j}$, $C^{(0)j}$, and $C^{(1)j}$ are adjustable ion-interaction parameters that depend on temperature and pressure [63]. The constant, A_j is the Debye-Hückel parameter at different temperatures [25]. The values of the Pitzer constants $\beta^{(0)j}$ and $\beta^{(1)j}$ for some electrolytes are reported by Pitzer [25].

Revised Helgeson-Kirkham-Flowers equation (HKF)

The semi-empirical model developed by HKF is another approach in which the standard thermodynamic properties of aqueous electrolyte solutions at increasing temperatures can be obtained. HKF developed equations for the determination of the apparent molal heat capacity, standard partial molal heat capacity at infinite dilution, entropy, enthalpy, and Gibbs free energy of aqueous species at a desirable temperature and pressure [61].

$$Cp_{\phi} = \overline{Cp}^{\circ}_{j,T} + \frac{I}{m}A_j\sqrt{I}\left(\left(1+\sqrt{I}\right)^{-1} - \frac{\varkappa}{3}\right) - 2.303RT^2m\left(v_+v_-\right)\left(\frac{2}{T}\left(\frac{\partial B}{\partial T}\right)_p + \left(\frac{\partial^2 B}{\partial T^2}\right)_p\right) \quad (47)$$

where, $\varkappa = \frac{3}{I^{1.5}}(1+\sqrt{I} - \frac{1}{1+\sqrt{I}} - 2\ln(1+\sqrt{I}))$

$$\overline{Cp}^{\circ}_{j,T,P} = c_{1,j} + \frac{c_{2,j}T}{(T-\theta_j)} - \left(\frac{\theta T\left(2a_{3,j}(P-P^{\circ}) + a_{4,j}\left(P^2-P^{\circ 2}\right)\right)}{(T-\theta_j)^3}\right) + \omega_j\, TX \quad (48)$$

At standard pressure (1 bar), the partial molal heat capacity of the species at a given temperature in Eq. (48) is reduced to Eq. (49).

$$\overline{Cp}^{\circ}_{j,T} = c_{1,j} + \frac{c_{2,j}T}{(T-\theta_j)} + \omega_j\, TX \quad (49)$$

The partial molal heat capacity of an ion or electrolyte as a function of temperature and pressure was also proposed by Shock et al. [64] as represented in Eq. (50).

$$\overline{Cp}^{\circ}_{j,T,P} = c_{1,j} + \frac{c_{2,j}T}{(T-\theta_j)^2} - \left(\frac{2T}{(T-\theta_j)^3}\right) \times \left(a_{3,j}(P-P^{\circ}) + a_{4,j}\ln\left(\frac{\psi+P}{\psi+P^{\circ}}\right)\right) + \omega_j\, TX + 2TY\left(\frac{\partial \omega_j}{\partial T}\right)_p - T\left(\frac{1}{\varepsilon_{T,\,P}} - 1\right)\left(\frac{\partial^2 \omega_j}{\partial T^2}\right)_p \quad (50)$$

At standard pressure, Eq. (50) is reduced to Eq. (51).

$$\overline{Cp}^{\circ}_{j,T} = c_{1,j} + \frac{c_{2,j}T}{(T-\theta_j)^2} + \omega_j\, TX + 2TY\left(\frac{\partial \omega_j}{\partial T}\right)_p - T\left(\frac{1}{\varepsilon_{T,\,P}} - 1\right)\left(\frac{\partial^2 \omega_j}{\partial T^2}\right)_p \quad (51)$$

where P° and P (bar) is the Pressure at the reference state (1 bar) and desired pressure of calculation. $c_{1,j}$, $c_{2,j}$, $c_{3,j}$, $c_{4,j}$, $a_{1,j}$, $a_{2,j}$, $a_{3,j}$, $a_{4,j}$ are temperature/pressure ionic-specific independent HKF parameters obtained by regression. ω_j is the born coefficient, ψ is the solvent-specific parameter (2600 bar) and T is the temperature (K). X, Y, and Z are the born functions with the S.I unit of (K^{-1}). θ_j (K) is the structural temperature unique for each species (j) in Eqs. (48) and (49). In the case of the report of Shock et al., [64] in Eqs. (50) and (51), θ_j is a constant = 219 K.

$$X = \frac{1}{\varepsilon_{T,\,P}}\left(\left(\frac{\partial^2 ln\varepsilon_{T,\,P}}{\partial T^2}\right)_P - \left(\frac{\partial ln\varepsilon_{T,\,P}}{\partial T}\right)^2_P\right) \quad (52)$$

$$Y = \frac{1}{\varepsilon_{T,\,P}}\left(\frac{\partial ln\varepsilon_{T,\,P}}{\partial T}\right)_P \equiv \frac{1}{\varepsilon_{T,\,P}}\left(\frac{(-1+a.\theta.\exp(b+a.T))}{\theta}\right) \quad (53)$$

$$Z_{P,\,T} = -\frac{1}{\varepsilon_{T,\,P}} \quad (54)$$

$\varepsilon_{T,\,P}$ is the dielectric constant of water. The values of a, b, T, and θ are as defined in Eq. (7).

The value of the born function X can be obtained by the partial derivation of Eq. (52). The value -3.16×10^{-7} K^{-1} at 25 °C was reported by Helgeson & Kirkham [51].

A comparison of the results obtained from the Cp models can be found in the supplement. The difficulty and inconsistency in obtaining a satisfactory $\overline{Cp}^{\circ}_{j}$ result has been a major problem in the computation of specific heat capacity. However, many researchers measured the specific heat of aqueous electrolyte solutions and few people have done this with sufficient precision to obtain reliable results for the apparent molal heat capacity of the solute [65].

An assumption was made that the heat capacities of individual ionic species at infinite dilution are additive [65]. According to the reports of Criss & Millero [66], Parker [65], and Abraham & Marcus [67], the $\overline{Cp}^{\circ}_{j}$ of the electrolytes can be determined additively. Depending on the electrolyte salt type, Eq. (55) can be used to obtain the values of the partial molal heat capacity if the values of $\overline{Cp}^{\circ}_{j,298.15\,K}$ for the components of the electrolyte's ionic species at 25 °C and zero molality are known.

General form (additively) [65]

$$\overline{Cp}^{\circ}_{(M^+X^-)} = v_+\overline{Cp}^{\circ}_{(M^+)} + v_-\overline{Cp}^{\circ}_{(X^-)} \quad (55)$$

where M^+ is the cation and X^- is the anion of the electrolyte compound. v_+ and v_- are the stoichiometry coefficient of the respective cation and anion of the compound.

Some electrolytes were observed to give inconsistent values from regression [61]. Using $\overline{Cp}^{\circ}_{MgSO_4}$ as a reference, due to the strong electrostatic interaction of Mg^{2+} and $SO_4{}^{2-}$ in water, the linearization approximation of the Debye-Hückel theory is unsatisfactory [68]. The effects of ion associations on different apparent molal properties can be established at different ionic strengths. This depends on the differences in their standard enthalpies, heat capacities, dissociation volume, and Gibbs free energies [61]. The abrupt change in the ion association interaction of $MgSO_4$ at low molality makes it impossible to obtain an accurate value of its apparent heat capacity by extrapolation. From the study of the heat capacity of aqueous magnesium sulphate by Phutela & Pitzer [68] and Archer & Rard [63], $\overline{Cp}^{\circ}_{MgSO_4}$ can be obtained with the following expression [63,68]:

$$\overline{Cp}^{\circ}_{MgSO_4} = \overline{Cp}^{\circ}_{MgCl_2} + \overline{Cp}^{\circ}_{Na_2SO_4} - 2\overline{Cp}^{\circ}_{NaCl} \quad (56)$$

$$\overline{Cp}^{\circ}_{MgSO_4} = \frac{q_1}{T} + q_2 + q_3T + q_4T^2 + q_5T^3 \quad (57)$$

$$\overline{Cp}^{\circ}_{solute} = -295.3 + s_1(T-298.15) + s_2\left(T^2-298.15^2\right) + s_3\left(T^3-298.15^3\right) \quad (58)$$

where $q_1 = -6.2543 \times 10^6$, $q_2 = 6.5277 \times 10^4$, $q_3 = -2.6044 \times 10^2$, $q_4 = 4.6930 \times 10^{-1}$ and $q_5 = -3.2656 \times 10^{-4}$ [68], $s_1 = -18.52779$, $s_2 = 0.0728295$ and $s_3 = -8.79539 \times 10^{-5}$ [63] are fitting parameters and T is the temperature (K).

The partial molal heat capacity of $MgSO_4$ at infinite dilution, which is temperature-dependent was computed by Phutela & Pitzer [68] with the expression in Eq. (57) arriving at $\overline{Cp}^{\circ}_{MgSO_4} = -287.54$ $J.mol^{-1}K^{-1}$ at 25 °C, 20 bar. Likewise, Archer & Rard [63] proposed Eq. (58) for the

Table 1
List of species and their thermodynamic data at standard state.

Species (j)	$\Delta G^{o}_{j,\ 298.15K}$	$\Delta H^{o}_{j,\ 298.15K}$	$S^{o}_{j,\ 298.15K}$	$Cp^{o}_{j,\ 298.15K}$	References
H^{+}	0	0	0	0	[39,80,81]
SO_4^{2-}	-744.00	-909.34	18.50	-254.54	[49]
	-744.63	-909.18	20.08	-234.91	[39,80]
	-744.46	-909.60	18.83	-269.37	[64]
Aluminium Species					
Al^{3+}	-483.70	-530.67	-325.10	-135.98	[1]
	-487.64	-538.40	-337.97	-122.65	[49]
	-485.34	-531.37	-321.75	32.62	[39]
	-485.00	-531.00	-325.10	-321.70	[81]
$AlSO_4^{+}$	-1245.40	-1430.90	-217.00	–	[1]
	-1249.74	-1428.87	-195.49	455.43	[49]
	-1247.09	-1430.97	-212.13	–	[39]
$Al(SO_4)_2^{-}$	-2000.70	-2338.90	-156.50	–	[1]
	-2002.55	-2336.89	-144.77	–	[39]
$Al_2(SO_4)_3^{\circ}$	–	–	–	–	[1]
	-3205.00	-3790.70	-583.25	–	[39]
	-3205.00	-3791.00	-583.20	–	[81]
Iron Species					
Fe^{2+}	-90.53	-90.00	-101.58	-27.16	[49]
	-91.50	-92.26	-105.86	-33.05	[64]
	-78.90	-89.10	-137.70	–	[81]
Fe^{3+}	-17.24	-49.58	-277.40	-142.67	[1]
	-16.28	-49.00	-278.44	-67.23	[49]
	-17.24	-49.58	-277.40	-77.82	[64]
	-4.60	-48.50	-315.90	31.01	[79]
$FeSO_4^{+}$	-785.44	-932.86	-91.20	41.75	[1]
	-784.54	-932.34	-91.37	–	[49]
	-772.80	-931.78	-129.70	131.00	[81]
$Fe(SO_4)^{2-}$	-1537.30	-1829.50	-4.57	–	[1]
	-1524.65	-1828.39	-43.07	-703.44	[79]
$FeHSO_4^{2+}$	-780.89	-895.78	18.44	–	[1]
	-774.44	-883.07	40.01	–	[49]
	-768.38	-894.29	-18.68	235.83	[79]
Fe2(SO4)3o	–	–	–	–	[1]
	-2243.00	-2825.04	-571.53	–	[79]
Fe_2O_3	-742.20	-824.20	87.40	103.85	[1]
	-744.25	-826.23	87.40	103.88	[49]
	-742.20	-824.20	87.40	103.85	[81]
Nickel Species					
Ni^{2+}	-45.37	-59.50	-148.20	-42.77	[49]
	-45.60	-54.00	-128.90	–	[81]
$NiSO_4^{\circ}$	-803.30	-949.30	-18.00	-109.10	[1]
	-803.30	-949.30	-18.00	–	[81]
Cobalt Species					
Co^{2+}	-55.59	-57.60	-107.40	-26.58	[49]
	-54.39	-58.16	-112.97	-32.64	[64]
	-54.40	-58.20	-113.00	–	[81]
$CoSO_4^{\circ}$	-812.78	-960.31	-22.77	-302.00	[1]
	-799.10	-967.30	-92.00	–	[81]
Manganese Species					
Mn^{2+}	-230.54	-221.33	-67.78	-11.41	[49]
	-230.54	-221.33	-67.78	-17.15	[64]
	-228.10	-220.75	-73.60	50.00	[81]
$MnSO_4^{\circ}$	-985.90	-1116.10	20.92	–	[1]
	-985.92	-1121.11	20.92	-87.66	[49]
	-985.70	-1115.90	36.40	–	[81]
Magnesium Species					
Mg^{2+}	-453.98	-465.96	-138.07	-22.34	[1]
	-455.38	-467.00	-137.00	-16.02	[49]
	-454.80	-466.85	-138.10	–	[81]
$MgSO_4^{\circ}$	-1215.90	-1373.40	-53.68	-82.51	[1]
	-1212.21	-1356.00	-7.10	–	[81]
$MgSO_4.H_2O$	-1437.10	-1610.40	126.36	133.89	[1]
	-1437.21	-1610.71	126.36	138.91	[49]
	-1428.70	-1602.10	126.40	–	[81]

fitting and calculation of the partial molal heat capacity of solutes at saturated pressure of the solution and obtained a value of $\overline{Cp}^{\circ}_{MgSO_4} = -295.3\ J.mol^{-1}K^{-1}$ at 25 °C, 1 bar. This observation pointed out pressure influence on the partial molal specific heat capacity obtained by calculation at infinite dilution. The pressure effect is less for finite concentrations on the order of 0.1 mol/kg [63].

Determination of the apparent molal heat capacity by other theoretical calculation

A semi-empirical equation in the form of a simplified Redlich-Rosenfeld-Meyer (RRM) type [56] is found to be useful for the fitting of most dilute solutions at molality less than 1 molal or ionic strength up to 1 $mol.kg^{-1}$ in the different studies on the specific heat capacity

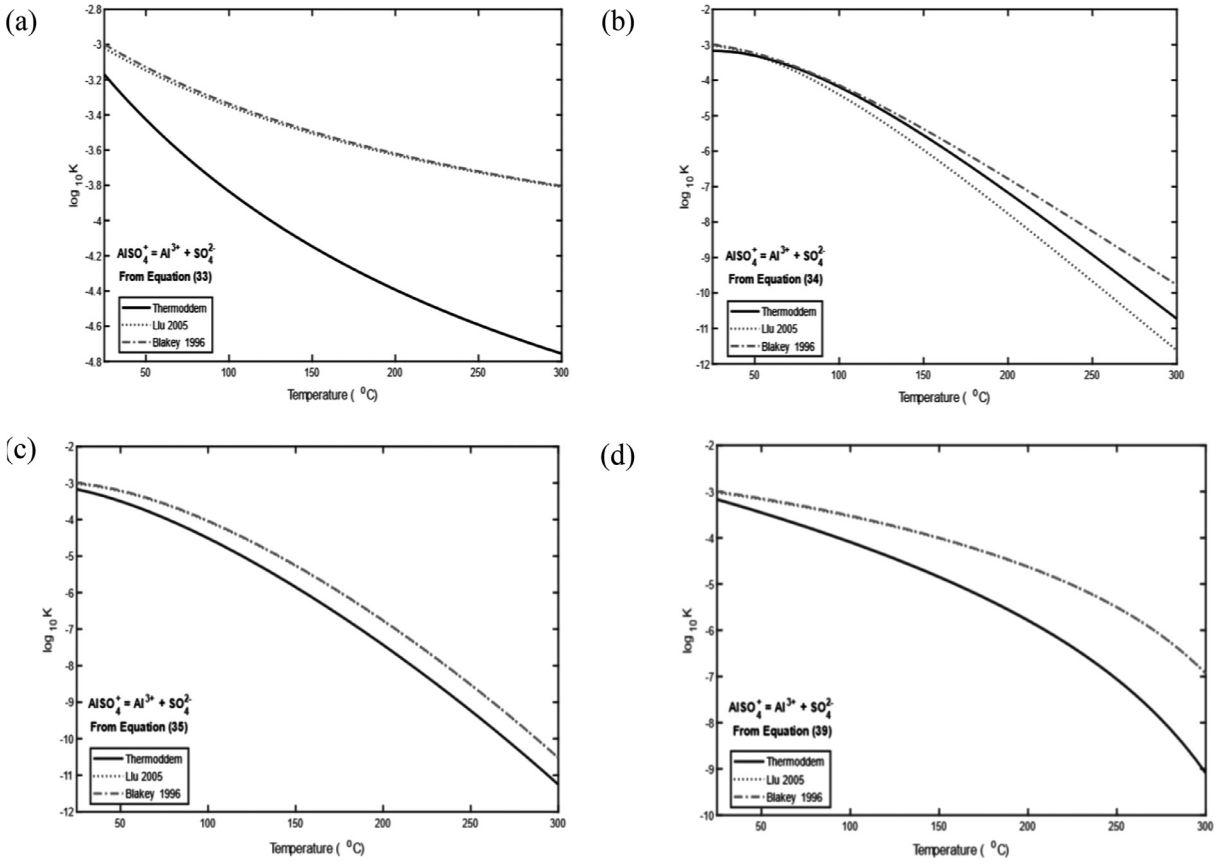

Fig. 1. Extrapolation of $\log(K_{i,T})$ for $AlSO_4^+ \Leftrightarrow Al^{3+} + SO_4^{2-}$ with thermodynamic data from 3 different sources [1,39,49] using (a) van't Hoff, (b) "Cp approximation", (c) Density and (d) Unexpanded HKF models.

measurement of electrolytes [55,62,67]. The apparent molal heat capacities of these dilute solutions of strong electrolytes are fitted with Eq. (59) [67] and Eq. (60) [55].

$$Cp_\phi = \overline{Cp}_j^\circ + \left(w \times S_{Cp} \times \sqrt{m}\right) + (b \times m) \tag{59}$$

$$Cp_\phi = \overline{Cp}_j^\circ + (w^{\frac{3}{2}}) A_c \sqrt{\rho_w} \times \sqrt{m} + (b \times w \times m) \tag{60}$$

The equation can also be represented as a function of only ionic strength [62] in the form:

$$Cp_\phi = \overline{Cp}_j^\circ + \left(S_{Cp} \times \sqrt{I}\right) + (b \times I) \tag{61}$$

A plot of "$Cp_\phi - (w^{\frac{3}{2}})A_c\sqrt{\rho_w} \times \sqrt{m}$" against "m" in Eq. (60) gives a straight-line graph, with a slope of b and an intercept at m = 0 being the value of $\overline{Cp}^\circ_{m=0}$ [55]. Woolley & Hepler [69] represented Eq. (60) as:

$$\frac{Cp_\phi - (1-\alpha)\overline{Cp}^\circ_{(M^{n+},X^{n-})} - (1-\alpha)^{1.5} A_c \sqrt{\rho_w} \times \sqrt{m}}{\alpha} = \overline{Cp}^\circ_{(MX)} + b\left(\frac{(1-\alpha)^2 m}{\alpha}\right) \tag{62}$$

where $\overline{Cp}^\circ_{(M^{n+},X^{n-})}$ can be determined from Eq. (56) for $MgSO_{4(aq)}$. α is the fraction of ions associated in $M^{n+}_{(aq)} + X^{n-}_{(aq)} \rightleftharpoons MX_{(aq,undissolved)}$. A plot of the left-hand side quantity versus the term in a bracket on the right-hand quantity of Eq. (62) gives a straight-line graph with an intercept $\overline{Cp}_j^\circ$ and the slope b [69].

The partial molal heat capacity $\overline{Cp}_j^\circ$ represents the value of the apparent molal heat capacity Cp_ϕ at infinite dilution (molality = 0). The valence factor $w = \frac{\text{Ionic strength}}{\text{molality}} = \sum \frac{v_i z_i^2}{2}$ (v_i is the subscript in the chemical formula $A_{v_+}B_{v_-}$ [60] and z_i is the charges on the ions), b is an empirical fitting adjustable parameter, and m is the molality. $S_{Cp} = w \times A_c\sqrt{\rho_w}$ is derived from the slope of the Debye-Hückel theory & the dielectric constant of water [21], ρ_w is the density of water ≈ 1 kg/dm^3. Different authors [65,70-72] have reported different values of $A_c\sqrt{\rho_w}$. The choice of the Debye-Hückel parameter used affects the $\overline{Cp}_j^\circ$ values obtained [55]. For salts of 1:1 electrolyte charge type, the value of $A_c\sqrt{\rho_w}$ has a very small impact on the calculated result of $\overline{Cp}_j^\circ$, but with a significant difference for higher electrolyte charge types. $A_c\sqrt{\rho_w}$ values have been reported by different authors at 25 °C to be 25.6 [65], 28.95 [72], 28.99 $J.K^{-1}mol^{-\frac{3}{2}}kg^{\frac{1}{2}}$ [70,71] and 32.75 $J.K^{-1}mol^{-\frac{3}{2}}kg^{\frac{1}{2}}$ [56,73] which is in good agreement with more recent data from Fernández et al., [74] with a 3% difference. The effect of pressure on the expression $A_c\sqrt{\rho_w}$ is minimal. This is confirmed by the values of $A_c\sqrt{\rho_w}$ reported by Archer & Wang [75] at different temperatures and pressures (31.89 at 25 °C, 1 bar, and 31.45 $J.K^{-1}mol^{-\frac{3}{2}}kg^{\frac{1}{2}}$ at 25 °C, 50 bar). The unit ($J.K^{-1}mol^{-\frac{3}{2}}kg^{\frac{1}{2}}$) does not reflect the litre in the density formula because, from the equation presented by Perron et al., [72], the full expression is $A_c(\frac{(\sqrt{\rho_w}\times\sqrt{m})}{c})$, where $m = 1\frac{mol}{kg}$ and $c = 1\frac{mol}{dm^3}$.

$A_c\sqrt{\rho_w}$ varies linearly with temperature (K). Perron et al., (1975) have suggested the use of Eq. (63) for the computation of the value which differs from the correlation of Millero [21] in Eq. (64). But the more recent values owing to the dielectric constant of water, revised by Archer & Wang [75] which is about 19% larger than that of Perron et al., [72] is assumed to be a "best" value [55].

$$A_c\sqrt{\rho_w}(T) = 28.95 + 0.325(T - 298.15) \tag{63}$$

$$A_c\sqrt{\rho_w}(T) = 31.8 + 0.464T \tag{64}$$

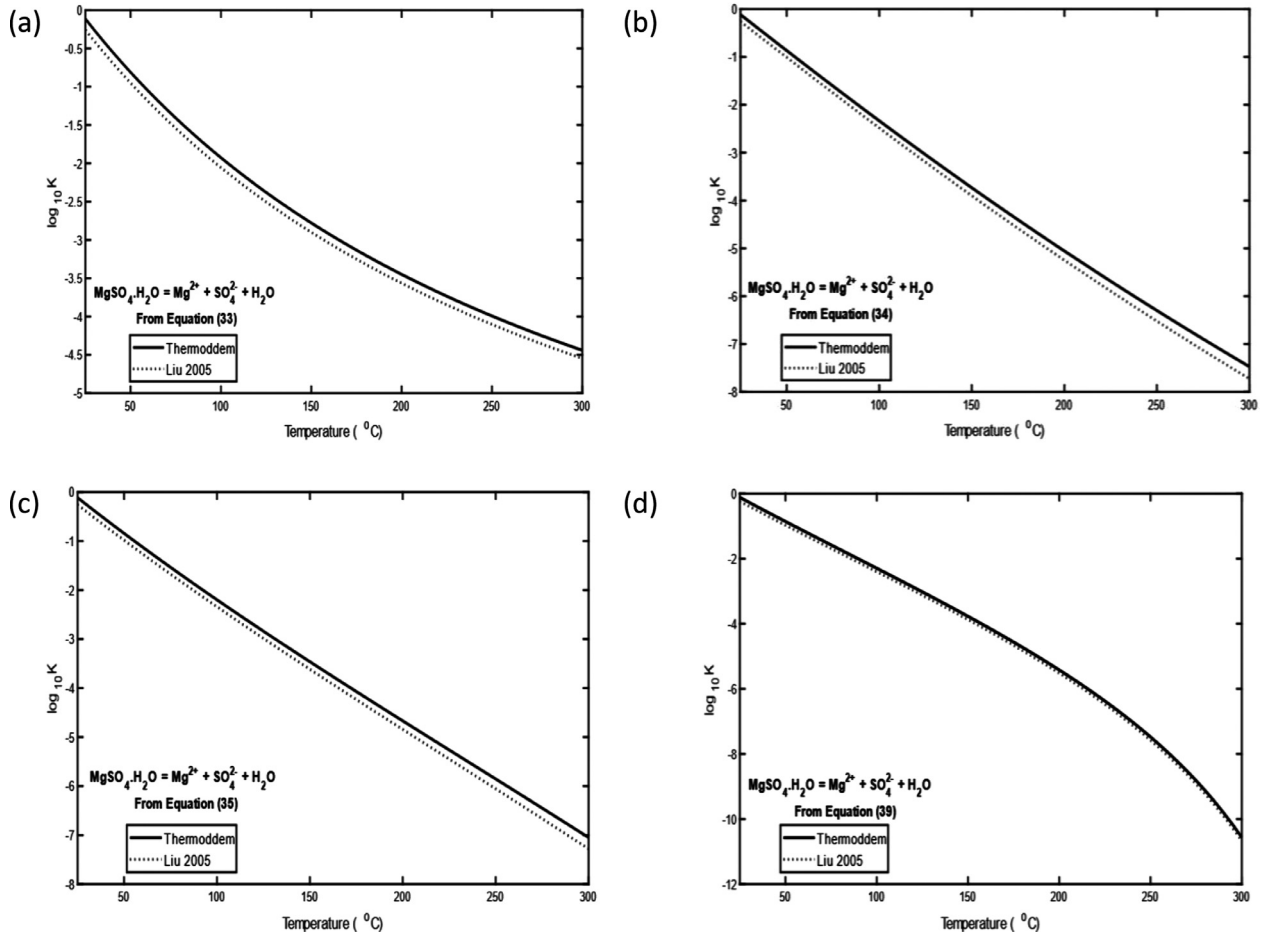

Fig. 2. Extrapolation of $\log(K_{i,T})$ for $MgSO_4.H_2O \Leftrightarrow Mg^{2+} + SO_4^{2-} + H_2O$ with thermodynamic data from 2 different sources [1,49] using (a) van't Hoff, (b) "Cp approximation", (c) Density and (d) Unexpanded HKF models.

The "T' in Eqs. (63) and (64) is the temperature in (K) and (°C) respectively. The Pitzer ion interaction equation so far is one of the best methods for computing the apparent heat capacity of many aqueous solutions [55,60,68] but the complexity of the equation and the unavailability of some data for various species has made the equation unattractive. Various researchers [63,75,76] have reported varying values for the parameters needed for the computation of some salt species such as $MgSO_4$ by fitting.

From the studies by different authors [58,68,77,78] and their comparisons, it is put forward that more accurate data are needed for the determination of the apparent molal heat capacity of many aqueous solutions in areas where the experimental data is unavailable. The apparent molal heat capacity of an aqueous species at 25 °C will be sufficient for the extrapolation of equilibrium constant with the models that utilise the specific heat capacity.

Methodology of the equilibrium constant extrapolation at high temperatures

In the aqueous chemical modelling study by Liu & Papangelakis [1], the equilibrium constants of eighteen dissociation reactions were computed with either the Density model, revised Helgeson-Kirkham-Flowers (HKF) model, or a regression method at three distinct temperatures of 230, 250 and 270 °C.

In this paper, the equilibrium constants of eleven out of these eighteen dissociation reactions for the Al-Mg-Fe-Ni-Co-Mn-H_2SO_4-H_2O system with complete thermodynamic data were extrapolated to higher temperatures using Eqs. (33), (34), (35), (40) and the unexpanded HKF model Eq. (39) or (41) for model comparisons. The remaining seven dissociation reactions obtained by the regression method [1] were not considered in this paper due to the unavailability of their thermodynamic data at the standard state of reference. The results obtained with Eqs. (39) and (41) are the same for species of a reaction with both negative values of enthalpy and entropy values. Hence, only values obtained from Eq. (39) were reported to avoid duplication. The thermodynamic data $\Delta G^{\circ}_{j,298.15\ K}$, $\Delta S^{\circ}_{j,298.15\ K}$, $\Delta H^{\circ}_{j,298.15\ K}$ and $\Delta C^{\circ}_{pj,\ 298.15\ K}$ of the species involved in the reactions were taken from four different sources Blakey & Papangelakis [39], Thermoddem database [49], Papangelakis & Demopoulos [79], and the report of Liu & Papangelakis [1] which is consistent with the thermodynamic documentations by Shock & Helgeson [40]. In cases where the heat capacity of a given species is not listed in the report of Liu & Papangelakis [1], data from Shock & Helgeson [40] or the Thermoddem database [49] having the values of $\Delta G^{\circ}_{j,298.15\ K}$, $\Delta S^{\circ}_{j,298.15\ K}$, $\Delta H^{\circ}_{j,298.15\ K}$ in close approximation to those reported by Liu & Papangelakis was used to enable the calculation of the equilibrium constant with models that require the specific heat capacity value. Otherwise, complete data from Papangelakis and Demopoulos [79] with the specific heat capacity value highlighted is used for the calculation of the equilibrium constants with the models that incorporate the heat capacity. Table 1 shows the lists of the considered species and their various thermodynamic data from different sources. To compare the effect of the thermodynamic data obtained from different sources, these values were used to extrapolate the equilibrium constants of the considered reactions at high temperatures.

In all cases, the term "Calculated-Liu" used in this paper is the value of the equilibrium constant $\log K_{i,T}$ obtained by Liu & Papangelakis

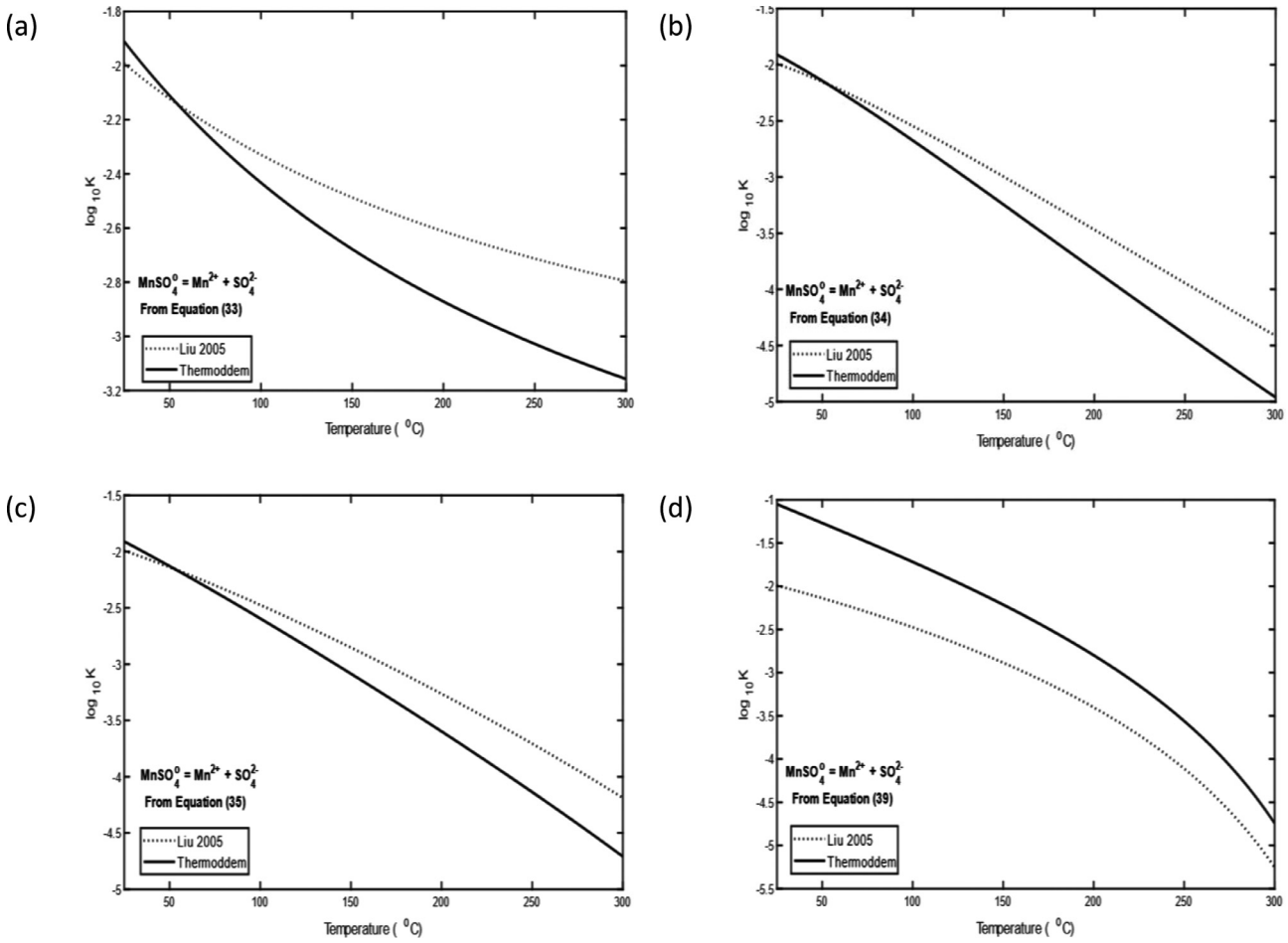

Fig. 3. Extrapolation of $\log(K_{i,\,T})$ for $MnSO_4{}^0 \Leftrightarrow Mn^{2+} + SO_4{}^{2-}$ with thermodynamic data from 2 different sources [1,49] using (a) van't Hoff, (b) "Cp approximation", (c) Density and (d) Unexpanded HKF models.

[1] at the three extrapolated temperatures (230, 250, and 270 °C) with either the Density, revised HKF model, or regression method. Regression was used by Liu & Papangelakis [1] for species without information on the thermodynamic data at the reference temperature. The regressed data were estimated with the equation $\ln K_T = A_1 + \frac{A_2}{T} + A_3T + A_4T^2$, where A_1, A_2, A_3, and A_4 are coefficients of the fit determined by regression or extrapolation, and T (K) is the temperature [1,82].

The terms "Liu 2005", "Blakey 1996", "Papangelakis 1990" and "Thermoddem" in Figs. 1–10 represent that the equilibrium constant was extrapolated from the thermodynamic data ($\Delta G^\circ_{j,298.15\ K}$, $\Delta S^\circ_{j,298.15\ K}$, $\Delta H^\circ_{j,298.15\ K}$ and $\Delta C^\circ_{pj,\ 298.15\ K}$) reported by Liu & Papangelakis [1], Blakey & Papangelakis [39], Papangelakis & Demopoulos [79], and the Thermoddem database [49] respectively. Eqs. (33), (34), (35), (40), and (39) are represented on the graphs as van't Hoff model, "Cp approximation" model, Density model, "Regressed experimental data" from the Thermoddem database and the unexpanded HKF model respectively. The species in the reactions presented in this paper with an index of zero indicates that it is an aqueous phase, e.g., $MgSO_4^o$ is the same as $MgSO_{4(aq)}$.

Results and discussion

Comparison of the equilibrium constants obtained by using thermodynamic data ($\Delta G^\circ_{j,298.15\ K}$, $\Delta S^\circ_{j,298.15\ K}$, $\Delta H^\circ_{j,298.15\ K}$ and $\Delta C^\circ_{pj,\ 298.15\ K}$) of reaction species from different sources

The sources of the thermodynamic data of the participating reaction species and the equilibrium constant models used for the extrapolation of the equilibrium constant influence the results. The differences observed in the modelling presented in Figs. 1–10 with data from 4 varying sources show the necessity for the acquisition of reliable thermodynamic data for the extrapolation of the equilibrium constant to elevated temperature.

Unlike data from the Thermoddem database [49], the extrapolation of $\log K_{i,\,T}$ with the thermodynamic data from Liu & Papangelakis [1] and Blakey & Papangelakis [39] for the $AlSO_4{}^+$ reaction are the same as seen in Fig. 1 (a, c, and d). There are noticeable differences in the $\log K_{i,\,T}$ results obtained in Fig. 1b with data from Liu & Papangelakis [1] and Blakey & Papangelakis [39] over the temperature range with the highest deviation of 16% at the highest studied temperature (300 °C).

For the $MgSO_4{\cdot}H_2O$ dissociation reaction, the results of $\log K_{i,\,T}$ computed with the thermodynamic data from the Thermoddem database and Liu & Papangelakis [1] using different equilibrium constant models in Fig. 2 show a close proximation with each other for the four computed models. In the case of $MnSO_4{}^\circ$ dissociation reaction, The comparison of the equilibrium constant of the species obtained with van't Hoff, "Cp approximation", Density and unexpanded HKF models in Fig. 3 using data from Liu & Papangelakis [1] and the Thermoddem database show a little difference at a lower temperature which increased with temperature for the van't Hoff, "Cp approximation" and the Density models contrarily to the unexpanded HKF model in Fig. 3d with a lower difference with increasing temperature.

The thermodynamic data at reference temperature for the $FeSO_4{}^+$ reaction as reported by Papangelakis & Demopoulos [79] and Liu & Papangelakis [1] were compared with the data from the Thermoddem

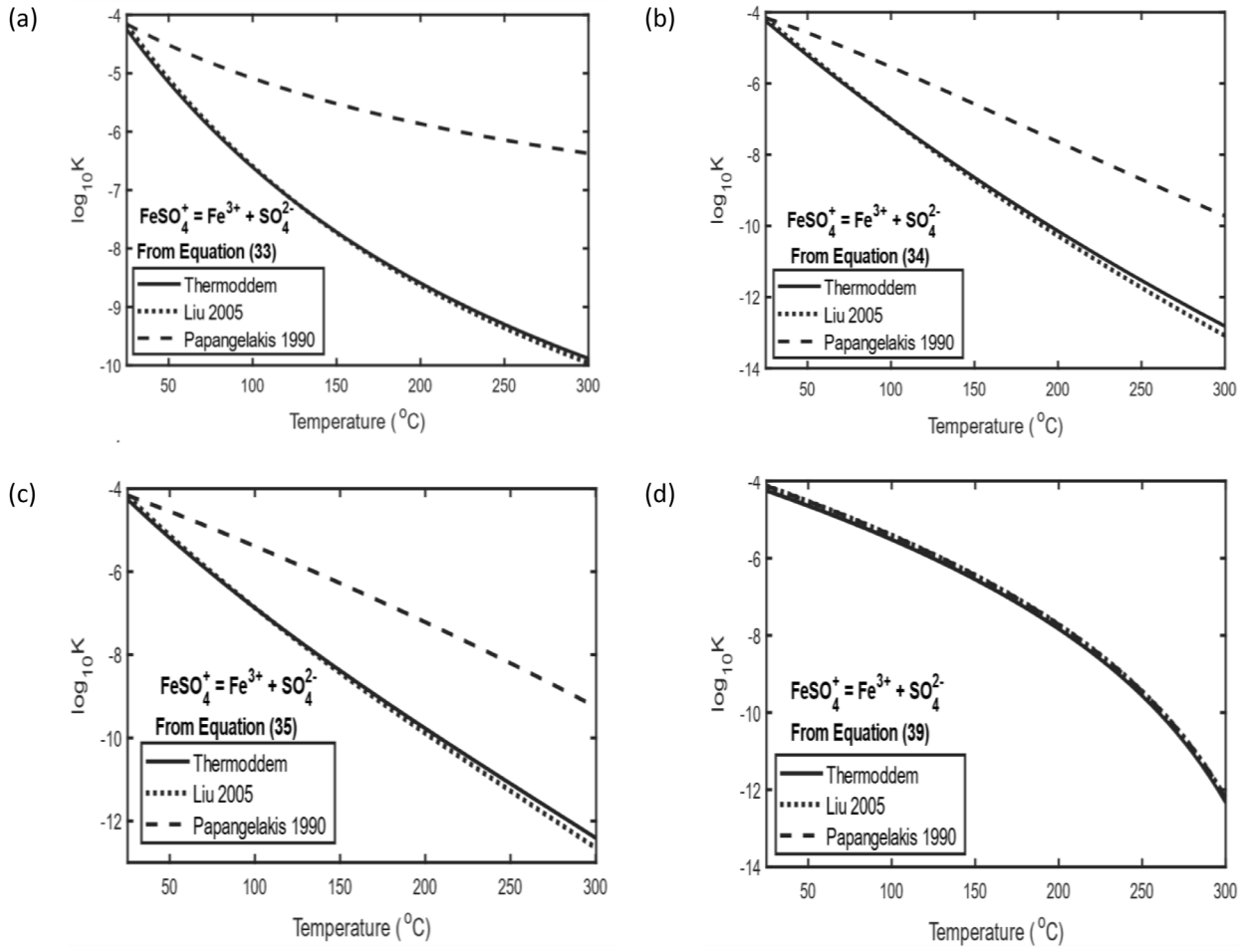

Fig. 4. Extrapolation of $\log(K_{i,T})$ for $FeSO_4^+ \Leftrightarrow Fe^{2+} + SO_4^{2-}$ with thermodynamic data from 3 different sources [1,49,79] using (a) van't Hoff, (b) "Cp approximation", (c) Density and (d) Unexpanded HKF models.

database. The values reported for SO_4^{2-}, Fe^{3+}, and $FeSO_4^+$ species by Papangelakis & Demopoulos [79] were used for the computation of "Papangelakis 1990″ in Fig. 4 while the values for SO_4^{2-}, Fe^{3+}, and $FeSO_4^+$ from Thermoddem [49] and Liu & Papangelakis [1] were used for $\log K_{i,T}$extrapolation for "Thermoddem" and "Liu 2005″ respectively. In this reaction, the results obtained from the calculation with the thermodynamic data from Thermoddem [49] and Liu & Papangelakis [1] are similar but different from the results obtained when the thermodynamic data reported by Papangelakis & Demopoulos [79] is used.

Considering the haematite reaction, there is a distinctive difference between the extrapolated values with the thermodynamic data ($\Delta G^\circ_{j,298.15\,K}$, $\Delta S^\circ_{j,298.15\,K}$, $\Delta H^\circ_{j,298.15\,K}$) of the participating species (Fe_2O_3, H^+, Fe^{3+}, and H_2O) obtained from the Thermoddem database [49] and Liu & Papangelakis [1] for the van't Hoff, "Cp approximation" and Density equilibrium constant models (Fig. 5 (a, b & c). While the unexpanded Helgeson model shows a negligible difference between the computed results with data from both sources (Fig. 5d).

Thermodynamic data from four literature sources were compared for $FeHSO_4^{2+}$ dissociation reaction. The equilibrium constant results obtained with data from Blakey & Papangelakis [39], Liu & Papangelakis [1], and Thermoddem [49] in Fig. 6(a & b) are similar with a little deviation at lower temperatures up to 150 °C, while the values obtained with the thermodynamic data from Papangelakis & Demopoulos [79] source shows a distinctive difference in comparison with the "Thermoddem", "Liu 2005" and "Blakey 1996" results.

The values of the thermodynamic data from Blakey & Papangelakis [39] and Liu & Papangelakis [1] used for the extrapolation of the equilibrium constant for $Al(SO_4)_2^-$ reaction (Fig. 7) shows a negligible difference in the results of the equilibrium constant. $Fe(SO_4)_2^-$ reaction in Fig. 8 shows that there is a vast difference in the $\log K_{i,T}$ across the temperature when the thermodynamic data from Liu & Papangelakis [1] is used in comparison with the data from Papangelakis & Demopoulos [79].

In a few cases such as in Figs. 9 and 10, there is a combination of thermodynamic data from two different sources where the complete data does not exist in one source. For the $NiSO_4^\circ$ dissociation reaction, the data ($\Delta G^\circ_{i,298.15\,K}$, $\Delta S^\circ_{i,298.15\,K}$and $\Delta C^\circ_{pi,\,298.15\,K}$) of Ni^{2+} from the Thermoddem database source [49] was used to complement the data from Liu & Papangelakis [1] for the equilibrium constants extrapolation in Fig. 9. On the other hand, the thermodynamic data for $NiSO_4^\circ$ from Liu & Papangelakis' report [1] was used to complement data from the Thermoddem source since the data for aqueous $NiSO_4^\circ$ is not reported in the Thermoddem database. The results obtained with data from both sources for the 4 equilibrium constant models approximate each other. On the other hand, for $CoSO_4^\circ \leftrightarrows Co^{2+} + SO_4^{2-}$ reaction, the thermodynamic data for $CoSO_4^\circ$ reported by Liu & Papangelakis [1] were used to complement the Co^{2+} and SO_4^{2-} data for the Thermoddem extrapolation since the data for aqueous $CoSO_4^\circ$ is not documented on the Thermoddem database. The data for Co^{2+} and SO_4^{2-} from Shock & Helgeson [40] which is consistent with the thermodynamic data used by Liu & Papangelakis [1] were used alongside the reported data of $CoSO_4^\circ$ for the calculation of "Liu 2005" in Fig. 10.

Unlike the $NiSO_4^\circ$ reaction, the equilibrium constant extrapolated from the combination of data from the 2 sources for the $CoSO_4^\circ$ reac-

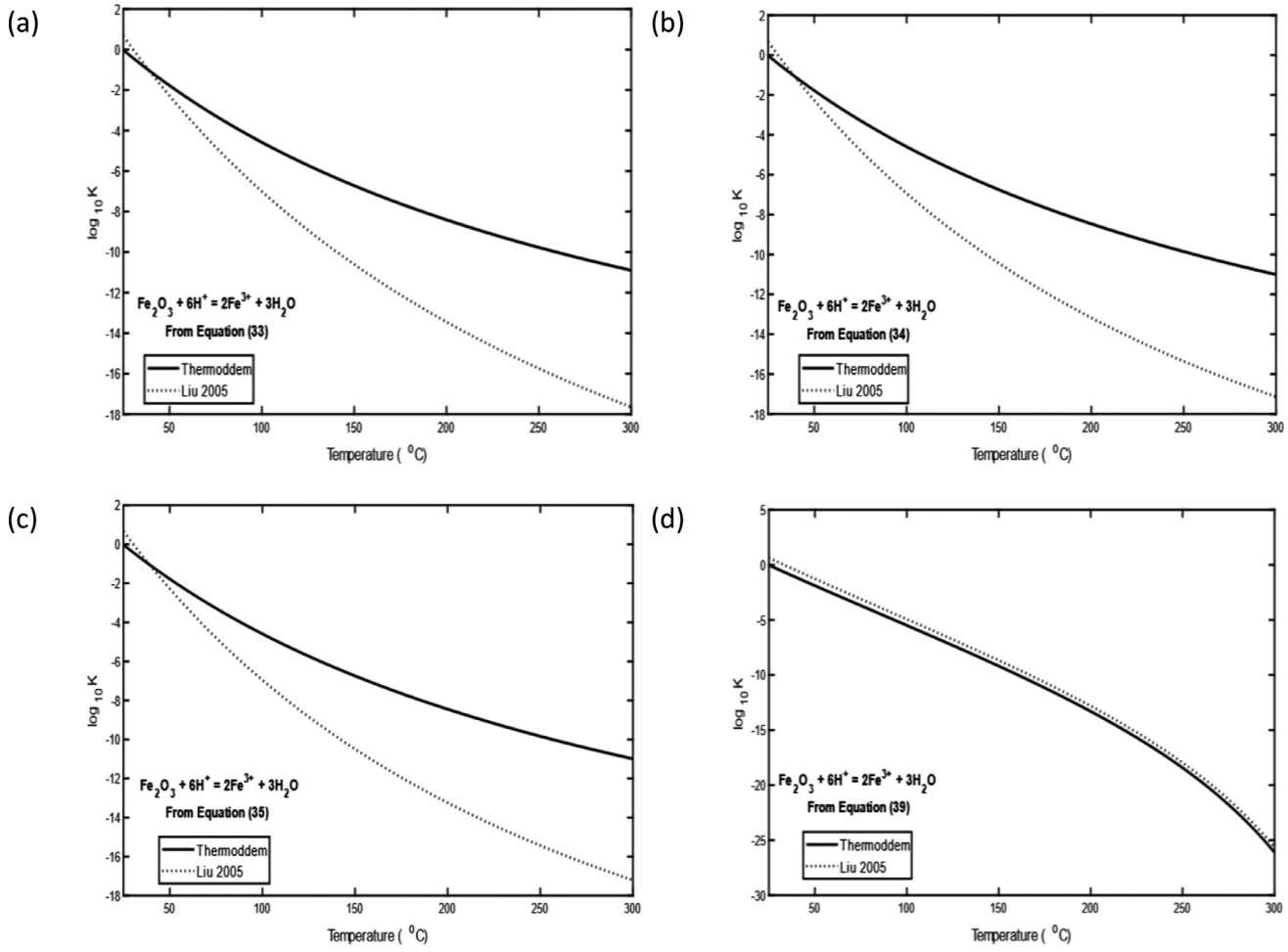

Fig. 5. Extrapolation of $\log(K_{i,T})$ for $Fe_2O_3 \Leftrightarrow 2Fe^{3+} + 3H_2O$ with thermodynamic data from 3 different sources [1,49,79] using (a) van't Hoff, (b) "Cp approximation", (c) Density and (d) Unexpanded HKF models.

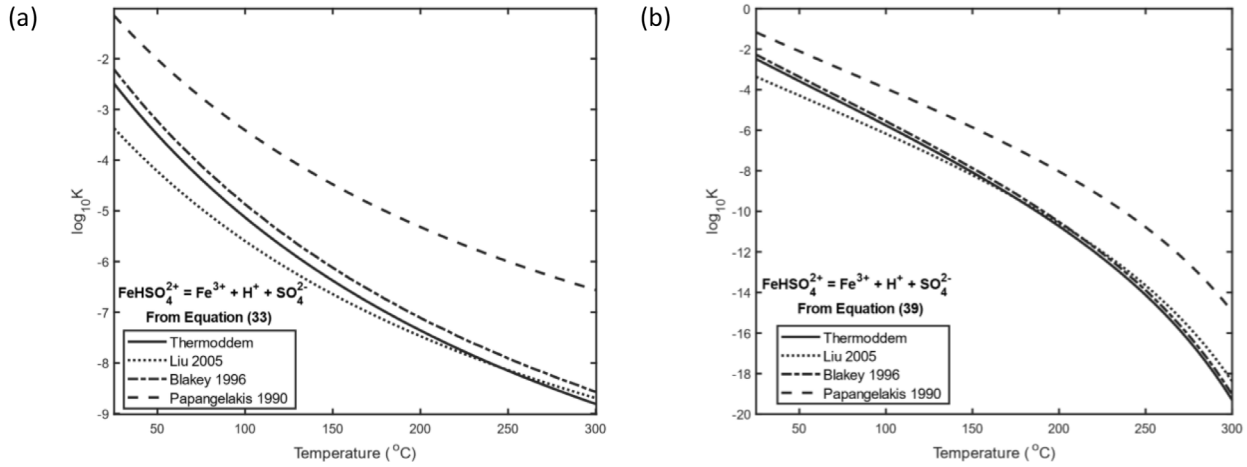

Fig. 6. Extrapolation of $\log(K_{i,T})$ for $FeHSO_4^{2+} \Leftrightarrow Fe^{3+} + H^+ + SO_4^{2-}$ with thermodynamic data from 4 different sources [1,39,49,79] using (a) van't Hoff, and (b) Unexpanded HKF models.

tion deviates from each other in all the considered models. This variation indicates the need for careful selection of thermodynamic data in completing the missing data from an intended reference source. Computation with data from one source would be preferred over the combination of inconsistent data from another source to minimize the error. The differences in the thermodynamic data in a source are linked to the methodology and condition used in determining it. Indeed, certain thermodynamic data are sometimes regressed without having any physical meaning.

The varying equilibrium constant results obtained using different equilibrium constant models with the thermodynamic data from the same source confirm the need for choosing a model with a

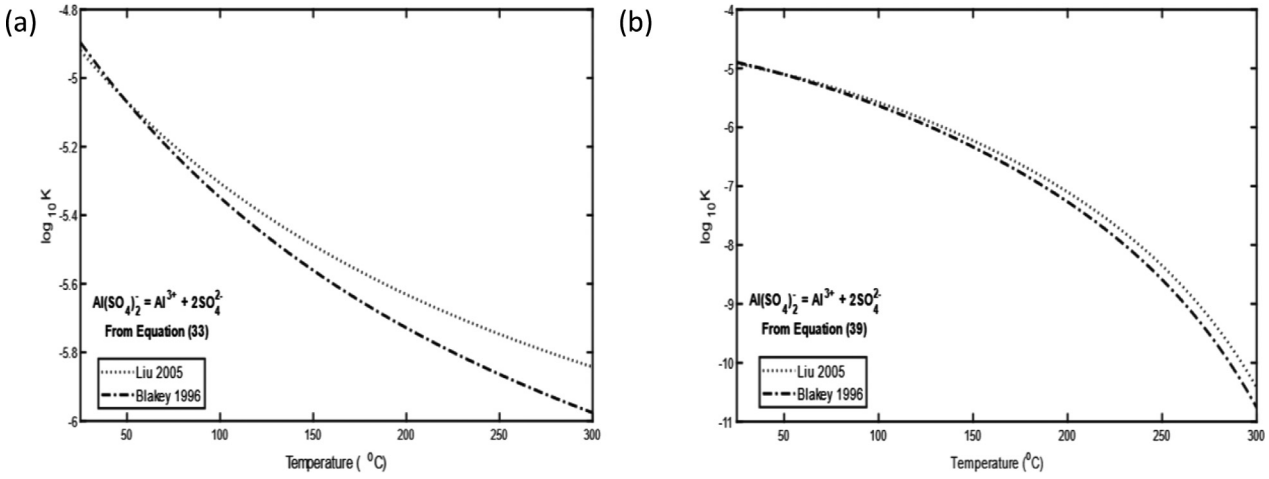

Fig. 7. Extrapolation of $\log(K_{i,T})$ for $Al(SO_4)_2^- \Leftrightarrow Al^{3+} + 2SO_4^{2-}$ with thermodynamic data from 2 different sources [1,39] using (a) van't Hoff, and (b) Unexpanded HKF models.

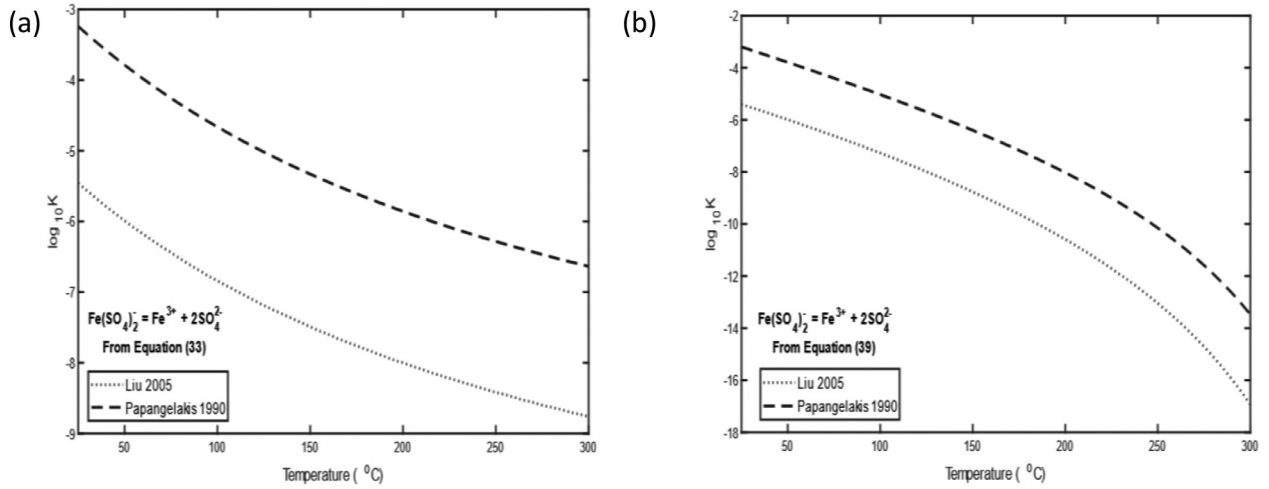

Fig. 8. Extrapolation of $\log(K_{i,T})$ for $Fe(SO_4)_2^- \Leftrightarrow Fe^{3+} + 2SO_4^{2-}$ with thermodynamic data from 2 different sources [1,79] using (a) van't Hoff, and (b) Unexpanded HKF models.

good assumption for the equilibrium constant calculation at higher temperatures.

Comparison of the calculated equilibrium constant from different models

Unless otherwise stated, the thermodynamic data from Liu and Papangelakis [1] were used for the calculation of the equilibrium constants of the reactions with Eqs. (33), (34), (35), and (39). The computed equilibrium constant values from the regressed experimental data in the Thermoddem database with Eq. (40) do not need thermodynamic data.

Contrary to the van't Hoff and unexpanded HKF model, the values of the extrapolated $\log K_{i,T}$ by the "Regressed experimental data", "Cp approximation" and the Density models in Fig. 11a show the same tendency with the equilibrium constants obtained by Liu & Papangelakis [1]. The results obtained from Eq. (40) which is based on empirical correlations with experimental data fitting were used as a base for the comparison of the studied model. As generally observed in the dissociation reactions considered, the deviation increases with temperature irrespective of the model used. The equilibrium constant models that consider the heat capacity of the reaction gave a result with a closer approximation to the regressed experimental data with a 10% deviation for both Density and "Cp approximation" models. While the unexpanded HKF and van't Hoff model deviates from the regressed experimental data by 41 and 68% respectively.

Similar to the $AlSO_4^+$ dissociation reaction, the regressed experimental data from Thermoddem, Density model, and "Cp approximation" model show a better propensity with the "Calculated-Liu" result than other models as seen in Fig. 11b. A comparison of the models with the regressed experimental data model in Fig. 11b shows that the "Cp approximation" model has the closest approximation to the regressed experimental data with the smallest deviation of 4% at the maximum temperature (300 °C). Consequently, the Density model shows a smaller deviation of 10% compared to the van't Hoff model with a 44% deviation. At lower temperatures up to 95 °C, van't Hoff's model aligned with the results from other models but deviates greatly as temperature further elevates. Thus, the van't Hoff model is strictly valid only at low concentrations and over a small temperature range. The effect of $\Delta C^\circ_{pi,298.15} = 0$ on $\log(K_{i,T})$ depends on the value of $\Delta H^\circ_{i,298.15}$ to a large extent. Since $\Delta H^\circ_{i,298.15}$ is relatively small for most dissociation reactions, the value of $\Delta C^\circ_{pi,298.15}$ cannot be ignored to avoid errors. But in the case where $\Delta H^\circ_{i,298.15}$ value is large as seen in polyphase reactions involving solids, the neglection of $\Delta C^\circ_{pi,298.15}$ is not noticeable so the assumption that $\Delta C^\circ_{pi,298.15} = 0$ gives a close value approximation to $\log(K_{i,T})$ [29]. The unexpanded HKF model is consistent with the models that take into account the specific heat capacity for the $MgSO_4.H_2O$ reaction. This model equally shows a close approximation with the regressed experimental data up to 180 °C and deviates further with temperature with a maximum value of 39% deviation at 300 °C.

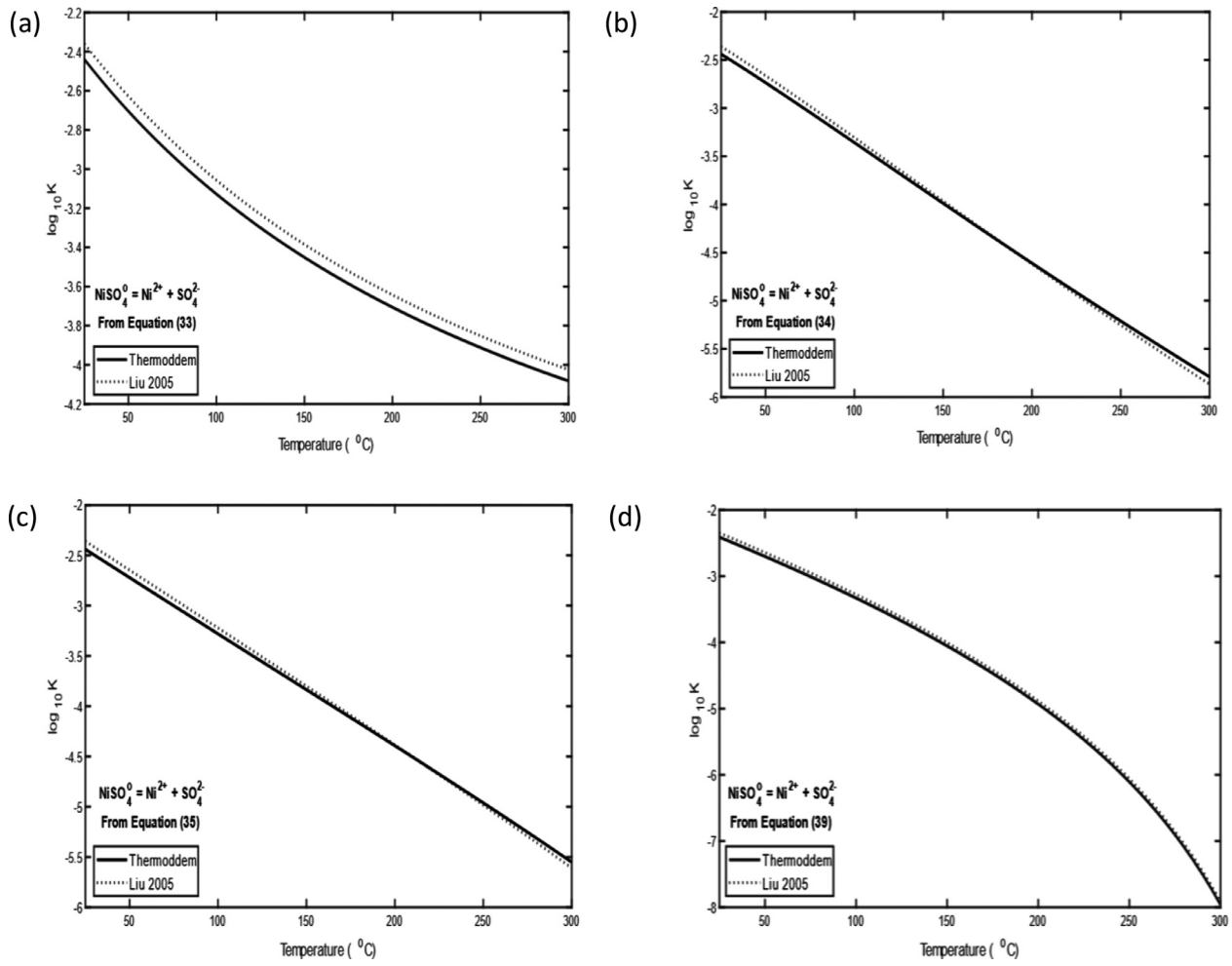

Fig. 9. Extrapolation of $\log(K_{i,T})$ for $NiSO_4^0 \Leftrightarrow Ni^{2+} + SO_4^{2-}$ with thermodynamic data from 2 different sources [1,49] using (a) van't Hoff, (b) "Cp approximation", (c) Density and (d) Unexpanded HKF models.

A comparison of the equilibrium constant models with the regressed experimental data in Fig. 11c shows that the "Cp approximation" and Density models gave the best approximation with respective deviations of 11 and 15% while the van't Hoff and unexpanded HKF model show a higher deviation by 39 and 20% respectively at the maximum studied temperature 300 °C. In Fig. 11d, the van't Hoff's model for the $CoSO_4^\circ$ reaction is consistent with the Density and "Cp approximation" models over the studied temperature range and shows a close approximation with data obtained by Liu & Papangelakis [1]. Comparing the equilibrium constant models with the results obtained from the experimental regression model, the least deviation of 2% is observed in the unexpanded HKF model while the "Cp approximation", Density and van't Hoff models deviate by 46% from the reported regressed experimental result in the Thermoddem database [49].

As seen in Fig. 11e, the van't Hoff model significantly deviates as temperature increased from 100 °C. Comparing the results of the models obtained with the regressed experimental data from the Thermoddem database at the most deviated temperature (300 °C), the van't Hoff model gave the highest deviation of 43% while the Density and "Cp approximation" and unexpanded HKF models deviate by 14, 10 and 4% respectively.

The accuracy of the thermodynamic equilibrium constant is dependent on the model used for the extrapolation. Depending on the model used, there is a vast difference between the calculated values obtained with the given thermodynamic data as the temperatures increase. In Fig. 11f ($FeSO_4^+$ reaction), the equilibrium constant calculated from the Density, "Cp approximation", van't Hoff and the unexpanded HKF models deviate greatly with temperature from the regressed experimental data by 39, 41, 22, and 36% respectively at the highest studied temperature (300 °C). Care should be taken that the data of the aqueous form of magnesium sulphate ($MgSO_4^\circ \equiv MgSO_{4(aq)}$) which is different from the thermodynamic data of the crystal form ($MgSO_{4(s)}$) was used in the modelling for $MgSO_4^\circ$ dissociation reaction. The results from the five models used for this calculation were compared as seen in Fig. 11g. The deviations observed in the considered equilibrium constant models from the regressed experimental data decreased with temperature. At 300 °C, the unexpanded HKF model deviates by 3% while the "Cp approximation", Density, and van't Hoff models deviate by 4, 9, and 40% respectively.

For the $FeHSO_4^{2+}$ reaction, the value of the specific heat capacity for the $FeHSO_4^{2+}$ species was not reported by Liu & Papangelakis [1]. Hence, the Density and "Cp approximation" models were computed from the thermodynamic data reported by Papangelakis and Demopoulos [79] with the heat capacity value for $FeHSO_4^{2+}$, while the van't Hoff and Helgeson models were obtained using data from Liu & Papangelakis, [1]. The discrepancy between the Density & "Cp approximation" model and the van't Hoff & unexpanded HKF model at a lower temperature (25 °C) in Fig. 11h is due to the varying thermodynamic data from both sources. The "Cp approximation" and Density model show the least deviation from the regressed experimental data at the maximum deviation of 300 °C by 4 and 10% respectively while the van't Hoff and unexpanded HKF model have a higher deviation corresponding to 28 and 35%.

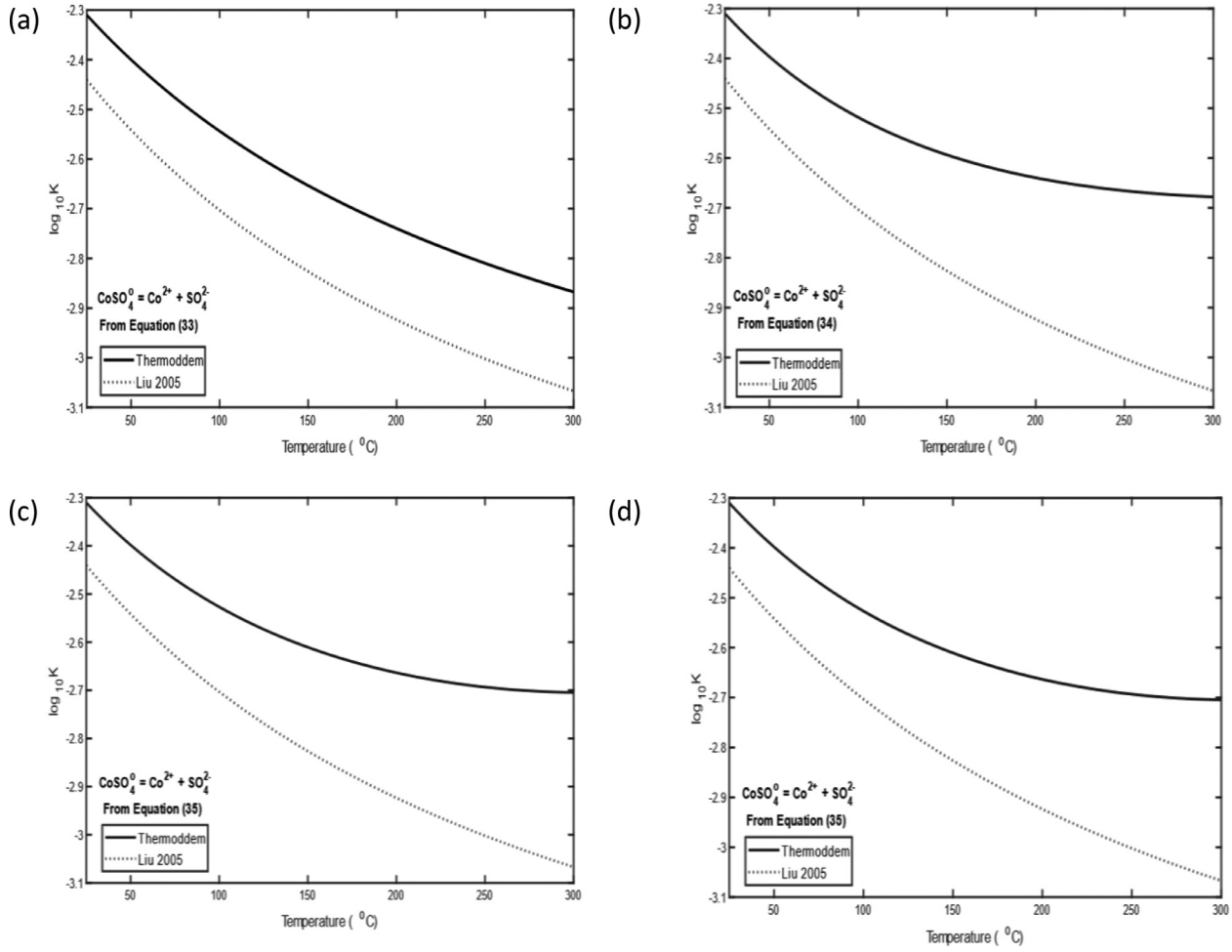

Fig. 10. Extrapolation of $\log(K_{i,T})$ for $CoSO_4{}^0 \Leftrightarrow Co^{2+} + SO_4{}^{2-}$ with thermodynamic data from 2 different sources [1,49] using (a) van't Hoff, (b) "Cp approximation", (c) Density and (d) Unexpanded HKF models.

Due to the absence of the specific heat capacity data for $Al(SO_4)_2{}^-$species in the literature, only van't Hoff and the unexpanded Helgeson models were used for the $Al(SO_4)_2{}^-$ dissociation reaction equilibrium constant modelling. Likewise, the thermodynamic data and experimental parameters for $Al(SO_4)_2{}^-$ were not reported in the Thermoddem database, hence no correlation was made with Eq. (40). The calculated values obtained with the van't Hoff and unexpanded HKF models in Fig. 11i show a considerable similarity only at lower temperatures up to 100 °C but vary significantly as temperature increases.

Similar to $FeHSO_4{}^{2+}$ species, the thermodynamic data from Papangelakis & Demopoulos [79] which presents the heat capacity value of $Fe(SO_4)_2{}^-$ was used to model the Density and "Cp approximation" model, while the data from Liu & Papangelakis [1] was used for the van't Hoff and unexpanded HKF model. Since the thermodynamic data presented for the reference entropy and enthalpy for the reaction species are entirely different in both sources, the data for the specific heat capacity of $Fe(SO_4)_2{}^-$ species reported by Papangelakis & Demopoulos [79] was not used to complement the data from "Liu 2005″. Instead, the calculation with the Density and "Cp approximation" models was made in its entirety with the data from Papangelakis & Demopoulos [79]. The Density and "Cp approximation" models present an exact result for the $Fe(SO_4)_2{}^-$dissociation reaction in Fig. 11j. The discrepancies between the Density & "Cp approximation" model and the van't Hoff & unexpanded HKF model at a lower temperature (25 °C) in Fig. 11j is associated with the different thermodynamic data value from different sources used for the calculation unlike in the cases where only the data from one source Liu & Papangelakis [1] was used for all equilibrium constant models comparison. The source and methodology adopted in acquiring the thermodynamic data are very useful and influence the equilibrium constant of a reaction.

The results obtained in Fig. 11k are similar for the van't Hoff, "Cp approximation" and the Density models with respective deviations of 31, 29, and 30% from the regressed experimental data at the maximum temperature (300 °C). The unexpanded HKF model is most deviated from the regressed experimental data by 53% for the ferric oxide reaction.

In Fig. 11, the variation of the equilibrium constant results obtained at higher temperatures from different models specifies the necessity for the utilization of a valid model to compute the equilibrium constant of a given reaction at a higher temperature. It can be deduced that the specific heat capacity is crucial for thermodynamic data to be considered as far as higher temperature extrapolation is concerned. The variety of the equilibrium constant of some aqueous species obtained from different sources at specific temperatures as well as the values calculated in this paper using different models is shown in the appendix (Table A1).

Conclusion on the equilibrium constant extrapolation with different models

Since the available equilibrium constant models used to extrapolate equilibrium constants to high temperatures rely on different assumptions, the assumption based on the heat capacity is the main supposition that unifies these models. However, some models include parameters that account for high temperature and pressure effects as in the case of the revised HKF model which gives similar equilibrium constant results as the Density model at higher temperatures [1,44]. The results obtained

from the equilibrium constant models clearly show that there are inconsistent equilibrium constant values when different models are used due to the varying models' assumptions and their input correlated parameters. Comparison of the equilibrium constant results obtained from different models was based on the results of the equilibrium constant obtained with the experimental fitting model in Eq. (40). The Density and Cp approximation models yield similar and better results than other compared models considered at higher temperatures. This deviation is due to the model's consideration of the heat capacity of the aqueous species involved in the reactions. The heat capacity accounts for the effect of temperature increase in the reaction. As seen in Fig. 11, a deviation from the models becomes significant as the temperature increases. The Density model is particularly termed to be better than other models due to its simplicity (unlike the complex revised HKF model) and the model suggests a correspondence principle for heat capacities value as well as the properties of the solvent at reference temperature [43].

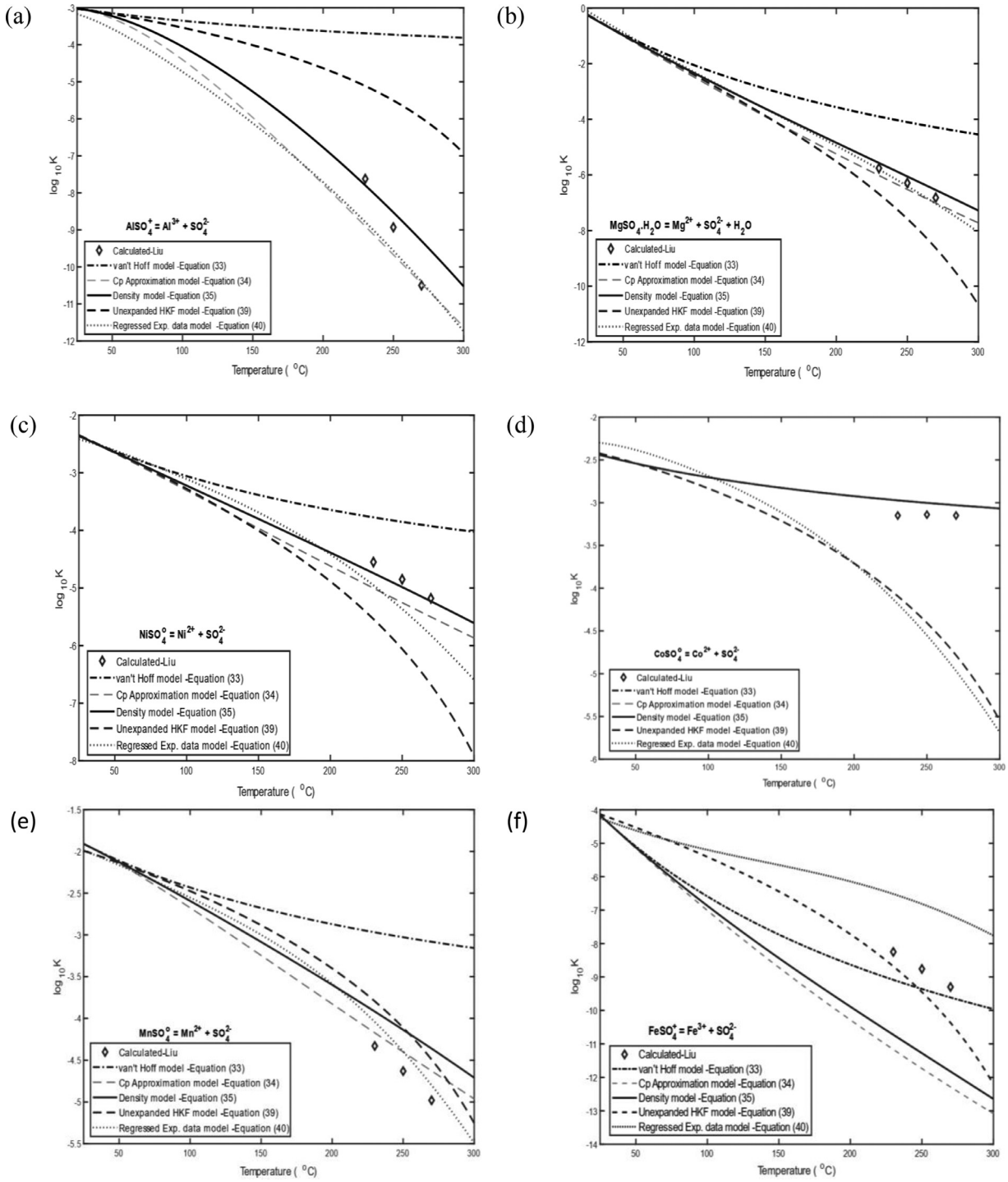

Fig. 11. Extrapolation of $\log(K_{i,T})$ for different reactions using the thermodynamic data from Liu & Papangelakis [1]. The Density and Cp approximation models for $FeSO_4^+$ and $FeHSO_4^+$ were extrapolated with data from Papangelakis & Demopoulos [79] with reported heat capacity data.
"Calculated-Liu" obtained with Density model in (a, b, g, h), "Calculated-Liu" obtained with Revised HKF model in (c, d, e, f), "Calculated-Liu" obtained with the Heat capacity of Fe_2O_3 + Revised HKF model of Fe^{3+} and H_2O in (k) as reported by Liu & Papangelakis [1].

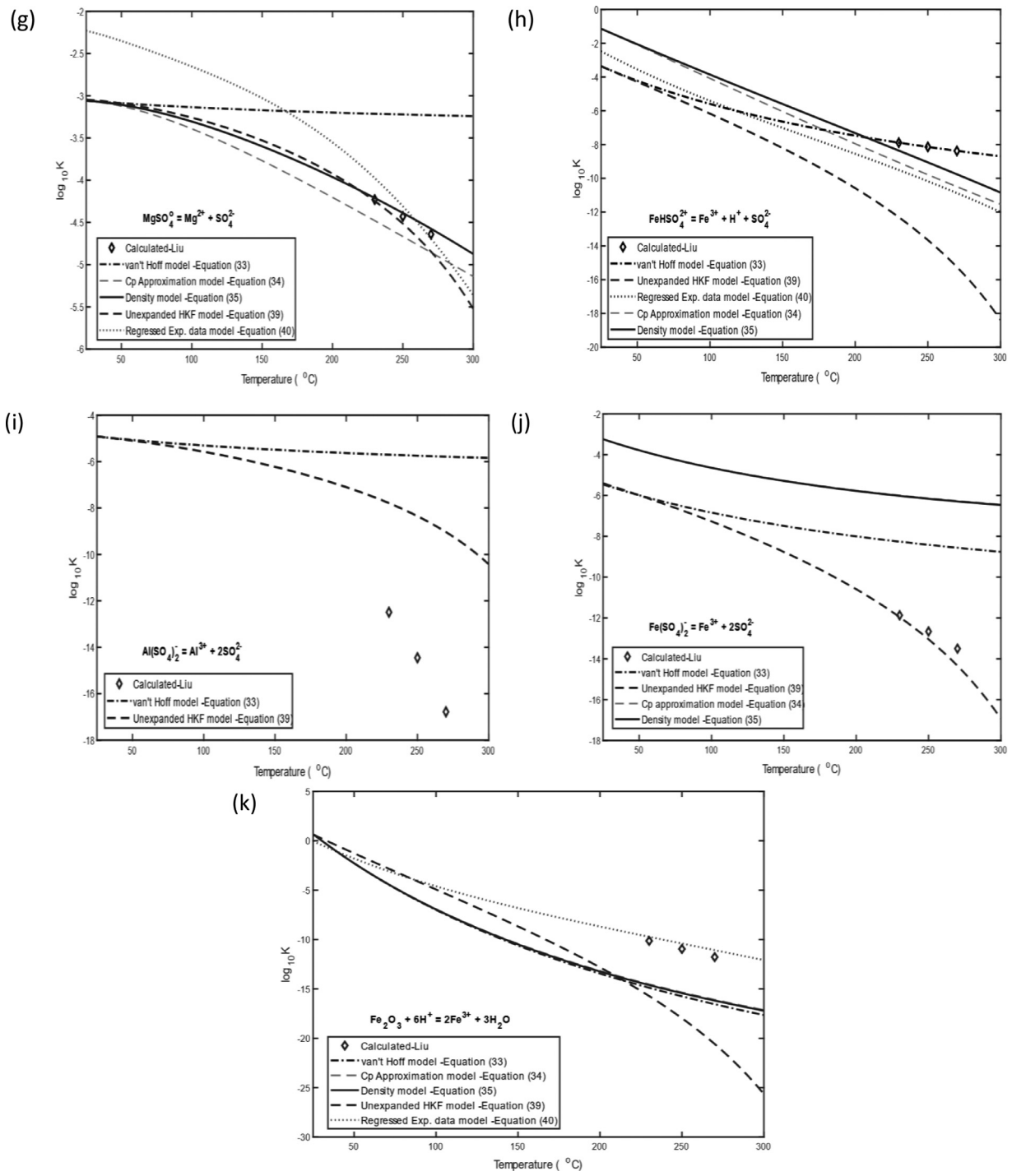

Fig. 11. Continued

The rationality of the Density model accuracy and the comparison with other equilibrium constant models is further tested in Section 8 with the speciation of hydronium alunite and kieserite formation.

Model validation (Case study)

Solution chemistry of aqueous species

Solubility data has been widely used to identify the chemistry and thermodynamics of aqueous solutions [83,84]. Due to the time and cost associated with solubility tests, precise thermodynamic modelling is a fundamental part of the development of hydrometallurgical processes [85].

Different software exists to solve equilibrium material balances, but most of this software has an old model with varying assumptions which are not suitable for high-temperature extrapolation of the equilibrium constant. A typical example of these models is the van't Hoff model which serves as the default thermodynamic database in the Phreeqc software and has to be modified to incorporate reliable computational models. This paper highlighted the discrepancies observed with various equilibrium constant models and in this section, the most suitable of these models for equilibrium constant calculation at high temperatures

is proven. This will guide users to decide on the best model to use for aqueous speciation modelling [86].

MATLAB software was used for the speciation calculations. The equilibrium constant and activity coefficient models were used to calculate the thermodynamic reaction constants with temperature.

The solubilities of aqueous species of $Al_2(SO_4)_3$ [84] and $MgSO_4$ [87] in H_2SO_4 (for a binary system) at 250 °C and 235, 270 & 300 °C respectively for aluminium and magnesium species were computed. To show the influence of the equilibrium constant and the activity coefficient models on the overall speciation, the equilibrium constants of Al-Mg-SO_4 species were determined by various engineering extrapolation methods with the models presented in Section 4.2. The data from three equilibrium constant models (Density, van't Hoff, and unexpanded HKF) were interchanged independently with the activity coefficient values obtained with Davies, Truesdell-Jones, and Bromley + Meissner models in the computation for comparison.

The Bromley activity coefficient model was combined with the Meissner activity coefficient model as stated in Eqs. (10) and (14) in other to account for the activity coefficients of the species at temperatures above 25 °C.

For the Truesdell-Jones activity coefficient model, the values of the parameter $\acute{\alpha}$ reported by Casas et al., [82] were used for some species not reported by Kielland [28]. The value of the ion size parameter $\acute{\alpha}$ is set to be 3 for neutral species such as $Al_2(SO_4)_3^{\circ}$ and $MgSO_4^{\circ}$, 4 for monovalent ions such as $AlSO_4^{+}$, and 4.5 Å for divalent ions. For HSO_4^{-}, the value of $\acute{\alpha}$ was obtained from the wateq4f.dat database on the Phreeqc software. The value of b_b for these species were kept constant with temperature which corresponds to 0.034 and 0.015 kg/mol at 250, and 300 °C respectively [82].

General approach and steps used for the speciation calculation of H_2SO_4-H_2O-$Al_2(SO_4)_3$-$MgSO_4$ with the MATLAB software

I. The equilibrium constants of the participating reactions were defined. The values of the equilibrium constants were calculated from the different equilibrium constant models specified in Eqs. (33), (35), (39), and (40) for $Al_2(SO_4)_3$ and $MgSO_4$ speciation.
II. The activity coefficients of the species were calculated from the different activity coefficient models specified in Eqs. (8), (9), and (10) + (14). The activity coefficient values obtained by Baghalha [94] from the Pitzer activity coefficient model were used directly for our computation for the Pitzer model comparison.
III. The "fsolve code on MATLAB software" was used to resolve the equations to determine the molar concentration of the unknowns Al^{3+}, $AlSO_4^{+}$, $Al_2(SO_4)_3^{\circ}$, Mg^{2+}, $MgSO_4^{\circ}$, HSO_4^{-}, H^{+} and SO_4^{2-} at each H_2SO_4 molal concentration for the aluminium and magnesium speciation considering the electroneutrality, ionic strength, and mass balance of the reaction species.

Cases for aluminium species H_2SO_4-$Al_2(SO_4)_3$ speciation at 250 °C

$H_2O \rightleftharpoons H^+ + OH^-$ (Rxn H_2O)
$HSO_4^- \rightleftharpoons H^+ + SO_4^{2-}$ (Rxn 1)
Aluminium species
$3AlSO_4^+ + 7H_2O \rightleftharpoons H_3OAl_3(SO_4)_2(OH)_{6(s)} + 4H^+ + HSO_4^-$ (Rxn 2)
$2AlSO_4^+ + HSO_4^- \rightleftharpoons Al_2(SO_4)_3^0{}_{(aq)} + H^+$ (Rxn 3)
$Al^{3+} + SO_4^{2-} \rightleftharpoons AlSO_4^+$ (Rxn 4)

Equilibrium constant expressions:

$$\text{From (Rxn } H_2O\text{)}; \quad K_{H_2O} = \frac{m_{H^+} \times \gamma_{H^+} \times m_{OH^-} \times \gamma_{OH^-}}{a_w}$$

$$\text{From (Rxn 1)}; \quad K_1 = \frac{m_{H^+} \times \gamma_{H^+} \times m_{SO_4^{2-}} \times \gamma_{SO_4^{2-}}}{m_{HSO_4^-} \times \gamma_{HSO_4^-}}$$

$$\text{From (Rxn 2)}; K_2 = \frac{m_{H^+}^4 \times \gamma_{H^+}^4 \times m_{HSO_4^-} \times \gamma_{HSO_4^-} \times a_{H-\text{Alunite}}}{m_{AlSO_4^+}^3 \times \gamma_{AlSO_4^+}^3 \times a_{\text{water}}^7}$$

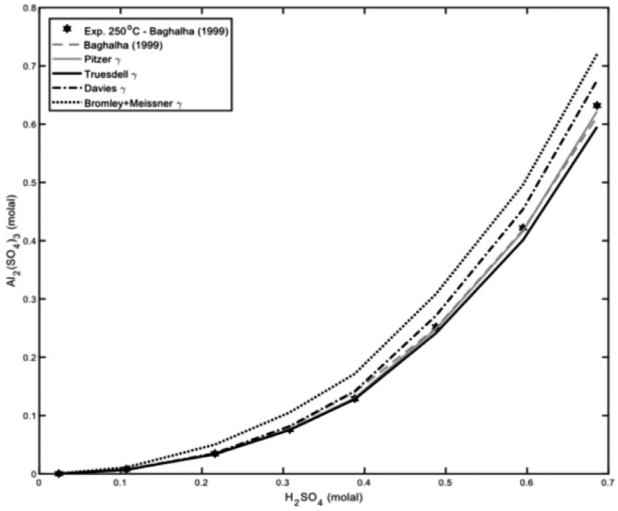

Fig. 12. Comparison of the experimental and calculated solubility of $Al_2(SO_4)_3$ with Pitzer, Truesdell-Jones, Davies, and Bromley + Meissner activity coefficient models at 250 °C. $\log(K_{H_2O})$, $\log(K_1)$ - $\log(K_4)$ used are as reported by Baghalha [84,94].

$$\text{From (Rxn 3)}; \quad K_3 = \frac{m_{Al_2(SO_4)_3^0}^{0} \times \gamma_{Al_2(SO_4)_3^0}^{0} \times m_{H^+} \times \gamma_{H^+}}{m_{AlSO_4^+}^2 \times \gamma_{AlSO_4^+}^2 \times m_{HSO_4^-} \times \gamma_{HSO_4^-}}$$

$$\text{From (Rxn 4)}; \quad K_4 = \frac{m_{AlSO_4^+} \times \gamma_{AlSO_4^+}}{m_{Al^{3+}} \times \gamma_{Al^{3+}} \times m_{SO_4^{2-}} \times \gamma_{SO_4^{2-}}}$$

Other governing equations are:

a. Electroneutrality:

$$mH^+ + (3 \times mAl^{3+}) + mAlSO_4^+ + (0 \times mAl_2(SO_4)_3^0) = mHSO_4^- + (2 \times mSO_4^{2-}) + mOH^-$$

b. Ionic strength:

$$I = 0.5 \times \left[mH^+ + (4 \times mSO_4^{2-}) + mHSO_4^- + mAlSO_4^+ + (9 \times Al^{3+}) + mOH^- + \left(mAl_2(SO_4)_3^{o}\right)^0\right]$$

c. Mass balance:

$$\text{Total sulphate} = m_{AlSO_4^+} + 3m_{Al_2(SO_4)_3^0} + m_{HSO_4^-} + m_{SO_4^{2-}}$$

$$\text{Total Aluminium} = \frac{m_{Al^{3+}} + m_{AlSO_4^+} + 2m_{Al_2(SO_4)_3^0}}{2}$$

The objective of this case study is to uniformly change and compare all the equilibrium constant values for the five reactions for each model respectively. But, due to the unavailability of reliable thermodynamic data ($\Delta H^{\circ}_{i,T}$, $S^{\circ}_{i,T}$ and $C^{\circ}_{p^{i,}\,T}$) for the hydronium alunite and neutral aluminium species reactions, it was not possible to obtain the values of $\log K_2$ and $\log K_3$ with the highlighted equilibrium constant models in this paper. The experimental solubility results used for the comparison of the calculated solubility data for hydronium alunite and kieserite formation are presented in Table 2.

Likewise, the equilibrium constant for water from Dickson et al., [95] was maintained, because the $\log K_{H_2O}$ was not reported in the regressed experimental model from the Thermoddem database. The values of $\log K_{H_2O}$, $\log K_1$ - $\log K_4$ used in Fig. 12 are as reported by Baghalha

Table 2
Experimental solubility data for common species in hydrometallurgical process at temperatures between $100 \leq T\ (°C) \leq 300$ in binary and ternary systems of sulphuric acid.

Species	System	T (°C)	H_2SO_4 (molal)	References
$Al_2(SO_4)_3$	$Al_2(SO_4)_3$-H_2SO_4	250	0 - 1.5	[84]
$Al_2(SO_4)_3$ and $MgSO_4$	$Al_2(SO_4)_3$-$MgSO_4$-H_2SO_4	250	0 - 1, 1.5	[82,84]
$MgSO_4$ (monohydrate)	$MgSO_4$-H_{2SO4}-H_{2O}	200, 235, 270, 300	0 - 2	[87]
Hematite solubility	Fe_{2O3}-H_{2SO4}-H_{2O}	230, 250, 270	0 - 0.8	[88]
$Fe_2(SO_4)_3$	Fe_2O_3-H_2SO_4-H_2O	150, 170, 185, 200	0.1 - 1	[89]
	$Fe_2(SO_4)_3$-H_2SO_4-H_2O	130, 150, 170, 230, 250, 270	0.1 - 0.7	[90]
Fe_2O_3 & $MgSO_4.H_2O$	$MgSO_4$-$Fe_2(SO_4)_3$-H_2SO_4 -H_2O	250	0.3 - 0.7	
$FeSO_4$	$FeSO_4$-H_2SO_4-H_2O	100	0 - 50*	[91]
		160, 180, 200, 220	0 - 0.52	[92]
$NiSO_4$ (Monohydrate)	$NiSO_4$-H_2SO_4-H_2O	200, 235, 270, 300	0 - 1.8	[93]

The acid concentration units are in molal except otherwise stated.
* was reported in% wt.

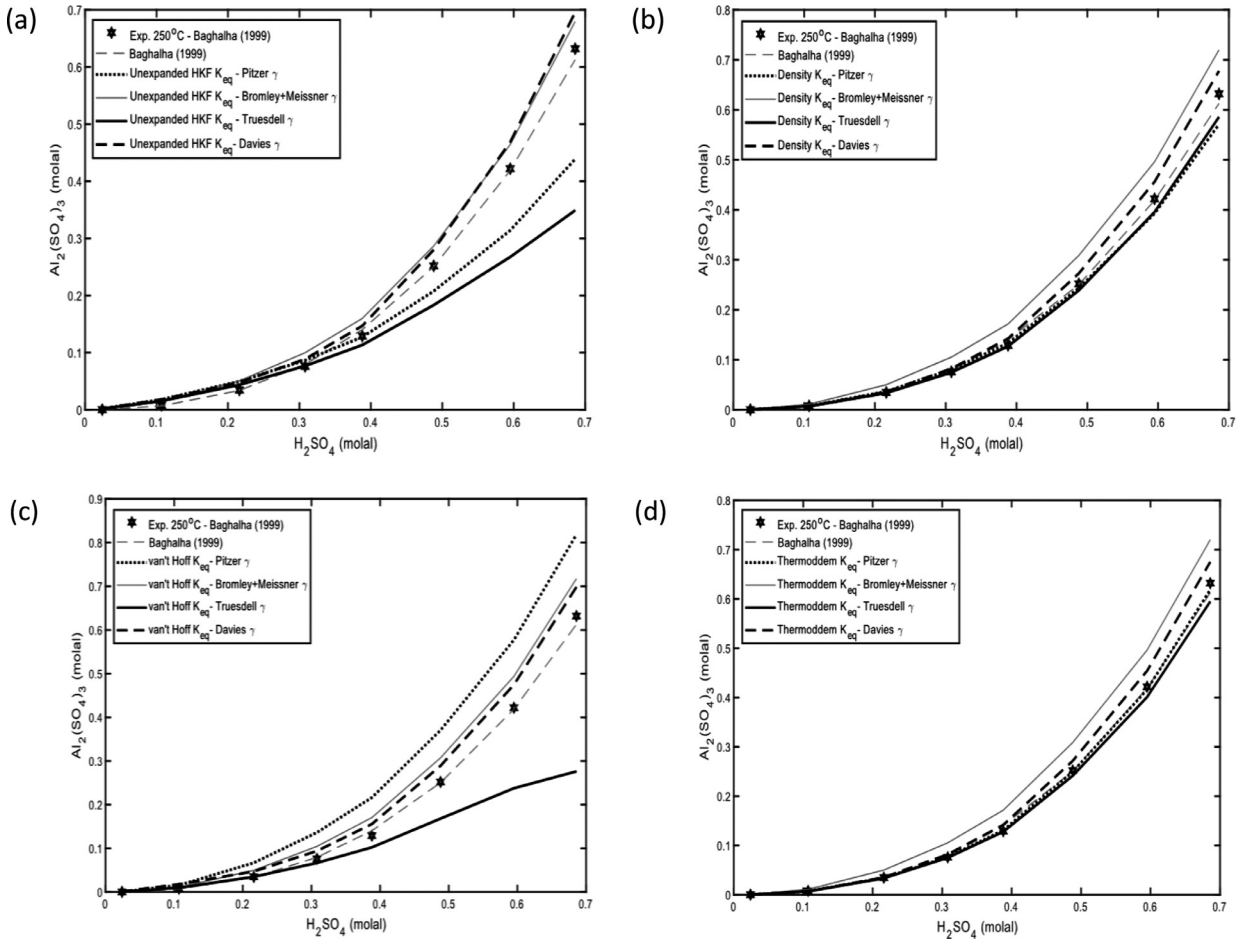

Fig. 13. Comparison of calculated solubility from equilibrium constant models (unexpanded HKF, Density, van't Hoff, Thermoddem) and activity coefficient models (Pitzer, Truesdell-Jones, Davies, Bromley + Meissner) with experimental and Baghalha [94] calculated solubility of $Al_2(SO_4)_3$ at 250 °C. $\log(K_{H_2O})$, $\log(K_1)$ and $\log(K_4)$ used are as reported by Baghalha [94], while $\log(K_2)$ and $\log(K_3)$ were calculated from the respective equilibrium constant models; (a) from Eq. (39), (b) from Eq. (35), (c) from Eq. (33) and (d) from Eq. (40).

& Papangelakis [84,94]. In Fig. 13 the equilibrium constants $\log K_2$ and $\log K_3$ could not be obtained with equilibrium constant models studied because there was no information about the thermodynamic data for the species $[Al_2(SO_4)_3^0]$ in (Rxn 2) and $[H_3OAl_3(SO_4)_2(OH)_6]$ in (Rxn 3). $\log K_1$ and $\log K_4$ values were obtained directly in each case from the calculation of the respective equilibrium constant models (unexpanded HKF, Density, van't Hoff, Thermoddem) used. The summary of the equilibrium constant values for the 5 reactions used for $Al_2(SO_4)_3$- H_2SO_4-H_2O speciation is presented in Table 3. The obtained solubility results from each case of the speciation calculation were compared with the experimental and the calculated solubility obtained by Baghalha & Papangelak [84,94]. The Pitzer activity coefficients (γ) values for the reaction species used in Fig. 12 were obtained by Baghalha [94] and his reported equilibrium constant values [$\log K_2$, $\log K_3$, $\log K_4$ fitted with the experimental data, $\log K_1$ (Dickson et al., [95]), and $\log K_{H_2O}$ (Marshal and Franck [96])].

As seen in Fig. 12, The solubility of $Al_2(SO_4)_3$ computed with the values provided by Baghalha [94] from the Pitzer model is similar to the values obtained by Baghalha [94] and fits best with the experimental data with better accuracy of 1.57% at the highest deviation point

Table 3
Equilibrium constant values of the reactions involved in the speciation of $Al_2(SO_4)_3$- H_2SO_4-H_2O system.

Models	Temperature (250 °C)				
	$\log(K_1)$ HSO_4^-	$\log(K_2)$ $H_3OAl_3(SO_4)_2(OH)_{6(s)}$	$\log(K_3)Al_2(SO_4)_3^{\circ}{}_{(aq)}$	$\log(K_4)$ $AlSO_4^+{}_{(aq)}$	$\log(K_{H_2O})$
van't Hoff	-1.995[V]	1.415[B]	2.523 [B]	3.727[V]	-11.191 [M]
Unexpanded HKF	-5.845[H]	1.415 [B]	2.523 [B]	5.730[H]	-11.191 [M]
Density	-5.827[E]	1.415 [B]	2.523 [B]	8.526[E]	-11.191 [M]
Thermoddem	-5.447[T]	1.415 [B]	2.523 [B]	9.564[T]	-11.191 [M]
Baghalla 1999	-5.355[D]	1.415 [B]	2.523 [B]	12.000 [B]	-11.191 [M]

All the equilibrium constant values from van't Hoff, Unexpanded HKF, and Density models were obtained with the thermodynamic data from Liu and Papangelakis [1] source which is consistent with Shock & Helgeson [40]. The Thermoddem data were extrapolated at the respective temperatures with Eq. (40) using the regressed experimental data from the Thermoddem database [49]. V: values calculated with the van't Hoff model Eq. (33), H: values obtained with the Unexpanded HKF model Eq. (39), E: values obtained with the Density model Eq. (35), T: values obtained with the Thermoddem model Eq. (40). B: data from Baghalha [94] fitted with the experimental data, D: data from Dickson et al., [95] used by Baghalha & Papangelakis [84,94], M: data from Marshall & Franck [96] used by Baghalha & Papangelakis [84,94].

of 0.686 molal H_2SO_4 compare to Baghalha [94] data with a difference of 3.04% to the experimental data. The Pitzer activity coefficient model aside from its complexity is established as the standard correlation for computing the electrolyte and osmotic coefficients of electrolyte solutions [97] owing to its validity at higher concentrations and ionic strengths and the consideration of the ion interaction (electrostatic and virial) [27,37,84]. The values obtained with the Bromley activity coefficient model while varying the equilibrium constant models show that the Thermoddem and Density models correspond with the van't Hoff model.

The solubility computed with the Truesdell-Jones activity coefficient model also shows a good agreement with the experimental data with a maximum deviation of 5.82%. The Davies activity coefficient model shows a good approximation up to 0.4 molal H_2SO_4 concentration and a higher deviation from the experimental data with the values of 6.38% at the highest H_2SO_4 concentration. The increase in deviation above 0.4 molal H_2SO_4 for the Davies model could be attributed to the fact that the equation is purely empirical and does not take into account the ion size parameter of the species which becomes significant as the concentration of the ionic species increases [32]. The combination of Bromley and Meissner which accounts for the ion interaction at higher temperatures presents the poorest fit with a maximum deviation of 12.23% to the experimental data.

Fig. 13 shows the solubility results when two of the equilibrium constants values ($\log K_1$ and $\log K_4$) are changed with the values obtained from the unexpanded HKF, Density, van't Hoff, and Thermoddem correspondingly. The Thermoddem and Density equilibrium constant models with the Truesdell-Jones activity coefficient model give the best fit to the experimental data. The results obtained from the computation of the solubility with the equilibrium constants from the unexpanded HKF and van't Hoff models with the various activity coefficients models show the greatest deviation from the experimental data with 44.76% for the unexpanded HKF model + Truesdell activity coefficient model, 56.29% for van't Hoff model + Truesdell-Jones activity coefficient model, 30.54% and 22.75% for unexpanded HKF model + Pitzer activity coefficient model and van't Hoff model + Pitzer activity coefficient model respectively.

Conclusion

In this case study, the Density, van't Hoff, unexpanded Helgeson models, and the regressed experimental data from the Thermoddem database [49] were used for the calculation of the equilibrium constants of the 5 reactions used in the thermodynamic speciation of the binary system of H_2SO_4-$Al_2(SO_4)_3$. Likewise, the activity coefficients of each participating species in the reactions were calculated from Truesdell-Jones, Davies, and the combination of Bromley + Meissner activity coefficient models. The results obtained with the combination of both models at 250 °C were compared with the experimental data of Baghalha & Papangelakis [84,94] and their computed models from the Pitzer activity coefficient model and fitting of the equilibrium constants. The Density and Thermoddem equilibrium constant models with the Truesdell-Jones activity coefficient model gave the best fit to the experimental data up to ionic strength of 4 molal. Instead of fitting the equilibrium constant from experimental data, the values of the activity coefficients obtained by Baghalha [94] using Pitzer activity coefficient models were combined with the equilibrium constant values calculated with the 4 equilibrium constant models used in this paper. The values obtained with the Density model and the regressed data values from Thermoddem Eq. (40) gave a result better than the fitted equilibrium constant models of Baghalha [94] (Table 4).

Cases for magnesium species (H_2SO_4-$MgSO_4$) speciation at 235, 270, and 300 °C

$H_2O \rightleftharpoons H^+ + OH^-$ (Rxn H_2O)
$HSO_4^- \rightleftharpoons H^+ + SO_4^{2-}$ (Rxn 1)
Magnesium species
$MgSO_{4(aq)}^{\circ} + H_2O \rightleftharpoons MgSO_4.H_2O$ (Rxn 5)
$Mg^{2+} + SO_4^{2-} \rightleftharpoons MgSO_4^{\circ}{}_{(aq)}$ (Rxn 6)

Equilibrium constant expressions:

$$\text{From } (\text{Rxn } H_2O);\ K_{H_2O} = \frac{m_{H^+} \times \gamma_{H^+} \times m_{OH^-} \times \gamma_{OH^-}}{a_w}$$

$$\text{From (Rxn 1)};\quad K_1 = \frac{m_{H^+} \times \gamma_{H^+} \times m_{SO_4^{2-}} \times \gamma_{SO_4^{2-}}}{m_{HSO_4^-} \times \gamma_{HSO_4^-}}$$

$$\text{From (Rxn 5)};\quad K_5 = \frac{a_{MgSO_4.H_2O_{(s)}}}{m_{MgSO_4^{\circ}} \times \gamma_{MgSO_4^{\circ}}}$$

$$\text{From (Rxn 6)};\quad K_6 = \frac{m_{MgSO_4^{\circ}} \times \gamma_{MgSO_4^{\circ}}}{m_{Mg^{2+}} \times \gamma_{Mg^{2+}} \times m_{SO_4^{2-}} \times \gamma_{SO_4^{2-}}}$$

Other governing equations are:

a. Electroneutrality

$$mH^+ + (2 \times mMg^{2+}) = mHSO_4^- + (2 \times mSO_4^{2-}) + mOH^-$$

b. Ionic strength

$$I = 0.5 \times [mH^+ + (4 \times mSO_4^{2-}) + mHSO_4^- + mOH^- + (4 \times Mg^{2+}) + (0 \times mMgSO_4^{\circ})]$$

c. Mass balance (Magnesium species)

$$\text{Total sulphate} = m_{MgSO_4^{\circ}} + m_{HSO_4^-} + m_{SO_4^{2-}}$$

$$\text{Total Magnesium} = m_{Mg^{2+}} + m_{MgSO_4^{\circ}}$$

Table 4
Equilibrium constant values of the species involved in the speciation of $MgSO_4$-H_2SO_4-H_2O system.

Equilibrium constants	Models	Temperatures (°C)			
		235	250	270	300
$\log(K_1)HSO_4^-$	Density	-5.526[E]	-5.827[E]	-6.240[E]	-6.886[E]
Reaction	U-HKF	-5.440[U]	-5.845[U]	-6.476[U]	-7.723[U]
	van't Hoff	-1.995[V]	-1.995[V]	-1.996[V]	-1.996[V]
	Baghalla 1999	-5.110[D]	-5.355[D]	-5.694[D]	-5.784[D]
$\log(K_5)$ $MgSO_4.H_2O$	Density	1.514[E]	1.667[E]	1.967[E]	2.407[E]
Reaction	U-HKF	2.585[U]	3.064[U]	3.785[U]	5.149[U]
	van't Hoff	-2.680[V]	-2.678[V]	-2.676[V]	-2.672[V]
	Baghalla 1999	1.664[B]	1.882[B]	2.173[B]	–
$\log(K_6)$ $MgSO_4^\circ$	Density	4.255[E]	4.388[E]	4.575E	4.874[E]
Reaction	U-HKF	4.308[U]	4.514[U]	4.844[U]	5.522[U]
	van't Hoff	3.218[V]	3.222[V]	3.230[V]	3.241[V]
	Baghalla 1999	4.454[B]	4.664[B]	4.944[B]	–
$\log(K_{H_2O})H_2O$	Density	-10.945[E]	-10.902[E]	-10.866[E]	-10.858[E]
Reaction	U-HKF	-11.313[U]	-11.395[U]	-11.588[U]	-12.129[U]
	van't Hoff	-9.962[V]	-9.798[V]	-9.593[V]	-9.312[V]
	Baghalla 1999	-11.200[M]	-11.191[M]	-11.240[M]	-11.406[M]

All the equilibrium constant values from van't Hoff, Unexpanded HKF, and Density models were obtained with the thermodynamic data from Liu and Papangelakis [1] source which is consistent with Shock & Helgeson [40]. V: values calculated with the van't Hoff model Eq. (33), U: values obtained with the Unexpanded HKF model Eq. (39), E: values obtained with the Density model Eq. (35), B: data from Baghalha [94], D: data from Dickson et al., 1990 used by Baghalha & Papangelakis [84,94], M: data from Marshall & Franck [96] used by Baghalha & Papangelakis [84,94].

In Fig. 14 (a & d), the values of $\log K_{H_2O}$, $\log K_1$, $\log K_2$, $\log K_5$ and $\log K_6$ used are as reported by Baghalha & Papangelakis [84,94]. The values of the $\log K_T$ of the 5 reactions used in the speciation of $MgSO_4$ in Fig. 14 (b, f & g) were calculated from the Density equilibrium constant model while the $\log K_T$ values used for Fig. 14 (c, e & h) were obtained from the unexpanded HKF model.

For Magnesium speciation, the results obtained when the van't Hoff equilibrium constants values were used gave results that are out of range irrespective of the temperature, with a large magnitude deviation in comparison with the experimental data, hence were not included in the figures.

The obtained results were compared with the experimental data of Marshall & Slusher [87] at 235, 270, and 300 °C and the calculated values of Baghalha [94] at 235 °C. No comparison was made by Baghalha [94] at 270 and 300 °C.

"Baghalha (1999) K_{eq}" in Fig. 14 signifies that all the $\log K_T$ values for the 5 reaction equations used for $MgSO_4$ speciation are the same as the values reported by Baghalha and Papangelakis [84,94].

The solubility result obtained when the equilibrium constants value from Baghalha [94] was used gave a poor fit to the experimental data for the three activity coefficient models used. Truesdell-Jones activity coefficient model gave the least deviation from the experimental data in Fig. 14(a & d) with a deviation of 29.97 and 36.97% at 235 and 270 °C respectively at the highest H_2SO_4 concentration. Similar to Fig. 14 (c, f & h), where the equilibrium constant values for the reactions were obtained from the unexpanded HKF model, there is a great deviation of the computed solubility values from the experimental data. The least deviated in this case (from Truesdell-Jones) activity coefficient model gives a maximum deviation of 56.87, 79.28, and 91.73% at 235, 270, and 300 °C respectively at the highest H_2SO_4 concentration.

Comparable to the aluminium speciation, the Truesdell-Jones activity coefficient model with the Density equilibrium constant model in Fig. 14 (b, e & g) shows the best fit with the experimental data. The maximum deviation when Truesdell-Jones and Density model is combined are 2.99, 3.41, and 5.21% at 235, 270, and 300 °C in the respective figures at the highest H_2SO_4 concentration. The Bromley and Davies in Fig. 14b at 235 °C yielded the same values while Baghalha [98] and Density-Truesdell models yielded the same values at 270 °C across the H_2SO_4 concentration.

The plots of the speciation molal distribution of the species involved in the $Al_2(SO_4)_3$_$MgSO_4$-H_2SO_4-H_2O reactions systems, pH, activity coefficients, and ionic strengths, using the results from the Density equilibrium constant models and the Truesdell-Jones activity coefficient model are documented in the paper supplement for comparison with the species distribution of the speciation calculations by Baghalha & Papangelakis [84,94].

Conclusion

In the case study of the binary system involving the speciation of H_2SO_4 - $MgSO_4$, the Density, and the unexpanded Helgeson models were used to calculate the equilibrium constant values of the 5 participating reactions. The values obtained with the van't Hoff model were completely out of range, hence it was not included in the report. The regressed experimental data from the Thermoddem database was not used because of the unavailability of some magnesium species needed for the calculation with Eq. (40). Correspondingly, the activity coefficients of each species in the reactions were calculated from Truesdell-Jones, Davies, and the combination of Bromley + Meissner activity coefficient models. The results obtained with the combination of both models at 235, 270, and 300 °C were compared with the experimental data of Marshal & Slusher [87]. Similar to the $Al_2(SO_4)_3$ speciation, the Density equilibrium constant models with the Truesdell-Jones activity coefficient model gave the best fit to the experimental data of $MgSO_4$.

General conclusion

This study shows that inconsistencies exist amongst the models used to calculate the speciation of aqueous electrolyte solutions at high temperatures up to 300 °C. This is mainly due to the models' assumptions and the thermodynamic data used to calculate the reaction equilibrium constants. Furthermore, it is important to note that there are relative differences between the thermodynamic data obtained from different sources in the literature for the extrapolation of the equilibrium constants. Depending on the reaction considered, this difference may or may not be significant over the entire temperature range. This study shows that the best results are obtained by considering the specific heat capacity of the compounds. The values obtained with the "Cp approximation" model (which assumes that $\Delta C^\circ_{pi,T}$ is constant) are very close

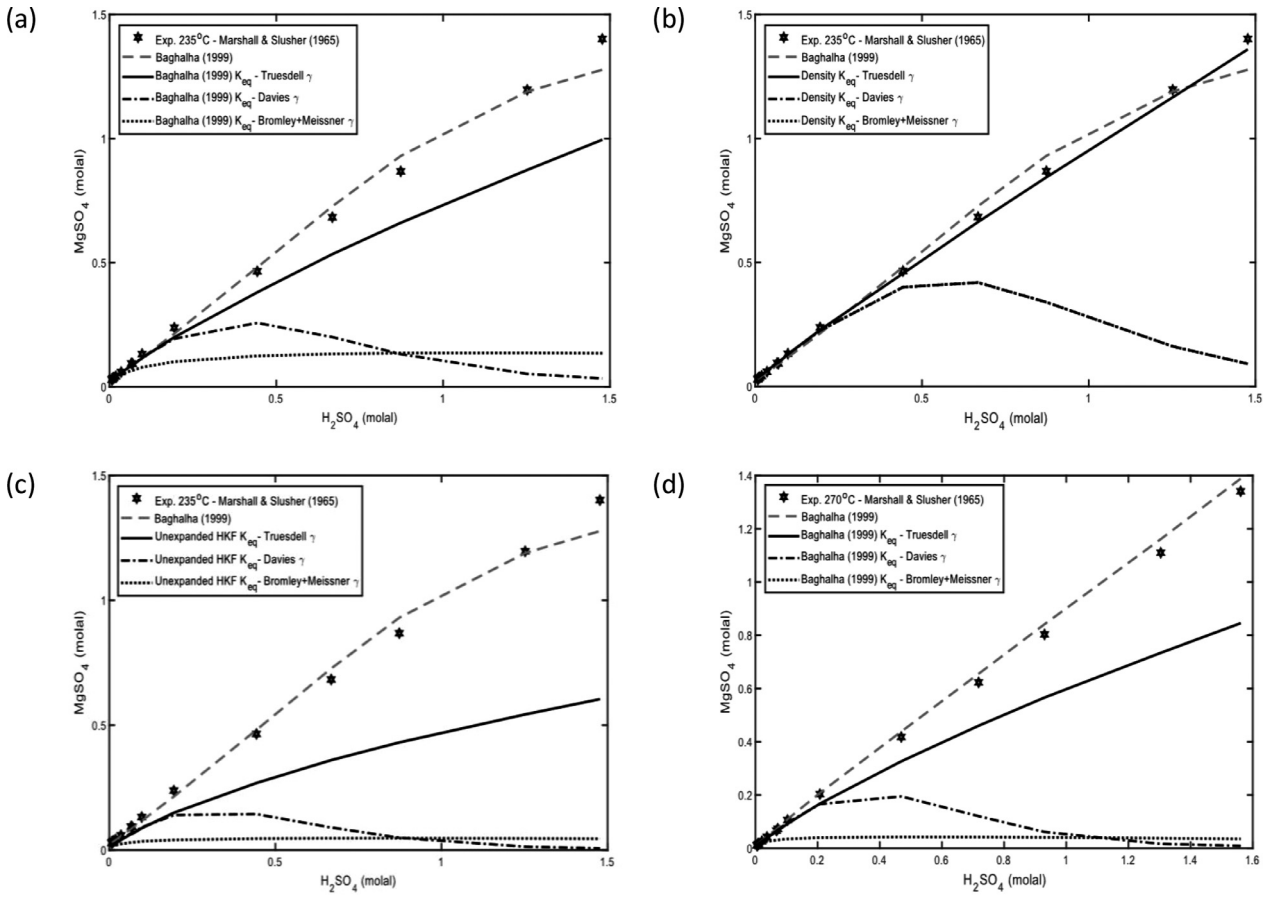

Fig. 14. Comparison of the experimental and calculated solubility of $MgSO_4$ at 235 °C (a, b & c), 270 °C (d, e & f), and 300 °C (g & h) with different activity coefficient models (Truesdell-Jones, Davies and Bromley + Meissner) and equilibrium constant models (Density and unexpanded HKF). (a, d) $\log(K_{H_2O})$, $\log(K_1)$, $\log(K_5)$ and $\log(K_6)$ used are as reported by Baghalha [94], (b, f, g) $\log(K_{H_2O})$, $\log(K_1)$, $\log(K_5)$ and $\log(K_6)$ used were calculated from the Density model, (c, e, h) $\log(K_{H_2O})$, $\log(K_1)$, $\log(K_5)$ and $\log(K_6)$ used were calculated from the Unexpanded HKF model.

to those from the Density model. The minimal differences could be attributed to the fact that the Density model also considers the density and thermal expansivity of the medium (e.g. water) in addition to the heat capacity (i.e. the expansion of the medium).

From studies [1,43,44], the revised HKF model has also been shown to provide the same accuracy as the Density model as long as the available low-temperature thermodynamic data are reliable. In contrast to the revised HKF model, the unexpanded HKF model does not give a very good estimate compared to the results obtained from the Density and "Cp approximation" models. The values deviate significantly with increasing temperature for most of the reaction species. This could be a reason for the improvement of the model by Helgeson [22,23,51]. It can be deduced that the specific heat capacity is an important thermodynamic fact to be taken into account concerning the extrapolation of the equilibrium constant with temperature.

From the speciation results of Aluminium and Magnesium species at their respective temperatures of 250 and 230, 270 & 300 °C, the Density and Thermoddem equilibrium constant models with the Truesdell-Jones activity coefficient model are best fitted to the experimental data and similar to results obtained with the Pitzer activity coefficient models by Baghalha and Papangelakis [84,94]. The estimation of $\log K_{i,T}$ with regressed experimental data from the "Thermoddem" database for most of the considered reactions shows good consistency with the Density model.

Finally, from the results obtained in this work, the unexpanded HKF and the van't Hoff equilibrium constant model would be the least recommended models to extrapolate the equilibrium constant at higher temperatures. Indeed, the assumption for van't Hoff that takes $\Delta C^{\circ}_{pi,298.15} = 0$ is invalid for the dissociation of most complexes and leads to errors when used to determine the value of the equilibrium constant ($\log(K_{i,T})$) at higher temperatures [25].

The obtained solubility results indicate that activity coefficients play an important role in the speciation of aqueous solutions, and the activity coefficient models that take into account the effects of ionic interactions are more appropriate to use [99]. The Truesdell-Jones activity coefficient gave results in close approximation with the Pitzer model even up to ionic strength of 4 mol/kg for this speciation with the Density and "Thermoddem" equilibrium constant models. From the literature [26], the Bromley activity coefficient model gives values similar to the Pitzer model at higher ionic strength, but the acquisition of the B parameter for this model is difficult since only the values at 25 °C are readily available. The combination of the Bromley and Meissner models to account for higher temperature speciation produced values that are higher than the experimental data with a deviation of 11.9 - 12.2% for aluminium species while the model gave a very poor value for magnesium species for all the equilibrium constant models considered with a relative percentage difference within the range of 64.4 - 99.3%.

Declaration of Competing Interest

The authors declare that they have no known competing financial interests or personal relationships that could have appeared to influence the work reported in this paper.

Data availability

Data will be made available on request.

Funding

This work was funded by the Association Nationale Recherche Technologie (ANRT-CIFRE) France, under grant [number 2021/1702].

Acknowledgments

The authors wish to thank Prony Resources, New Caledonia, Chaire MINAUMET - Mines Paris - PSL, and the Association Nationale Recherche Technologie (ANRT-CIFRE) France for supporting this study.

Supplementary materials

Supplementary material associated with this article can be found, in the online version, at doi:10.1016/j.ctta.2023.100117.

Appendix

Table A1
Comparison of the results of the equilibrium constant of some aqueous species in Liu & Papangelakis, [1] with other literature and the values calculated in this document.

Species (j)	Dissociation reactions (i)	Equilibrium constants $\log K_{i,T}$					Extrapolation method	Reference
		200 °C	230 °C	250 °C	270 °C	300 °C		
$AlSO_4^+$	$AlSO_4^+ = Al^{3+} + SO_4^{2-}$	–	-7.62	-8.93	-10.50	–	Eq. (35)	[1]
		-9.4	–	-12.0	–	-14.6	Regression	[84,98]
		-6.77	-7.80	-8.53	-9.30	-10.53	Eq. (35)	Calculated in this document
		-4.63	-5.11	-5.50	-5.98	-6.93	Eq. (39)	Calculated in this document
		-7.71	-8.79	-9.56	-10.39	-11.75	Eq. (40)	Calculated in this document
		-3.63	-3.69	-3.73	-3.76	-3.81	Eq. (33)	Calculated in this document
$Al(SO_4)^{2-}$	$Al(SO_4)_2^- = Al^{3+} + 2SO_4^{2-}$	–	-12.49	-14.45	-16.78	–	Eq. (35)	[1]
		-13.4	–	-17.4	–	-22.0	Regression	[98]
		-7.10	-7.79	-8.35	-9.03	-10.42	Eq. (39)	Calculated in this document
		-5.63	-5.70	-5.75	-5.79	-5.84	Eq. (33)	Calculated in this document
$MgSO_4^\circ$	$MgSO_4^\circ = Mg^{2+} + SO_4^{2-}$	–	-4.23	-4.43	-4.64	–	Eq. (35)	[1]
		-4.0	–	-4.6	–	-5.5	Regression	[84]
		-3.96	-4.48	-4.39	-4.58	-4.87	Eq. (35)	Calculated in this document
		-3.92	-4.25	-4.51	-4.85	-5.52	Eq. (39)	Calculated in this document
		-3.20	-3.21	-3.22	-3.23	-3.24	Eq. (33)	Calculated in this document
$MgSO_4.H_2O$	$MgSO_4.H_2O = Mg^{2+} + SO_4^{2-} + H_2O$	–	-5.76	-6.29	-6.82	–	Eq. (35)	[1]
		-5.2	–	-6.6	–	-8.1	Linear extrapolation	[82]
		-4.84	-5.57	-6.06	-6.54	-7.28	Eq. (35)	Calculated in this document
		-5.52	-6.68	-7.58	-8.63	-10.67	Eq. (39)	Calculated in this document
		-4.95	-5.80	-6.40	-7.03	-8.05	Eq. (40)	Calculated in this document
		-3.51	-3.90	-4.10	-4.29	-4.44	Eq. (33)	Calculated in this document
$MgHSO_4^{2+}$	$MgHSO_4^{2+} = Mg^{2+} + H^+ + SO_4^{2-}$	–	-6.94	-7.22	-7.48	–	Regression	[1]
		-5.3	–	-6.6	–	-7.9	Regression	[82]

References

[1] H. Liu, V.G. Papangelakis, Chemical modeling of high temperature aqueous processes, Hydrometallurgy 79 (1) (2005) Art. no. 1, doi:10.1016/j.hydromet.2003.10.014.

[2] B.I. Whittington, D. Muir, Pressure acid leaching of nickel laterites: a review, Miner. Process. Extr. Metall. Rev. 21 (6) (2000) 527–599, doi:10.1080/08827500008914177.

[3] T. Gultom, A. Sianipar, High pressure acid leaching: a newly introduced technology in Indonesia, IOP Conf. Ser. Earth Environ. Sci. 413 (2020) 012015, doi:10.1088/1755-1315/413/1/012015.

[4] P. Meshram, Abhilash, B.D. Pandey, Advanced review on extraction of nickel from primary and secondary sources, Miner. Process. Extr. Metall. Rev. 40 (3) (2019) 157–193, doi:10.1080/08827508.2018.1514300.

[5] K.A.K. Alibhai, A.W.L. Dudeney, D.J. Leak, S. Agatzini, P. Tzeferis, Bioleaching and bioprecipitation of nickel and iron from laterites, FEMS Microbiol. Rev. 11 (1–3) (1993) 87–95, doi:10.1111/j.1574-6976.1993.tb00271.x.

[6] C.K. Thubakgale, R.K.K. Mbaya, K. Kabongo, A study of atmospheric acid leaching of a South African nickel laterite, Miner. Eng. 54 (2013) 79–81, doi:10.1016/j.mineng.2013.04.006.

[7] E.C. Chou, P.B. Queneau, R.S. Rickard, Sulfuric acid pressure leaching of nickeliferous limonites, Metall. Trans. B 8 (4) (1977) 547–554, doi:10.1007/BF02669329.

[8] H. Liu, D.H. Rubisov, Solution chemistry and reactor modelling of the pal process: successes and challenges, Int. Laterite Nickel Symp. (2004) 289–305.

[9] M. Moldovan, E.M. Krupp, A.E. Holliday, O.F.X. Donard, High resolution sector field ICP-MS and multicollector ICP-MS as tools for trace metal speciation in environmental studies: a review, J. Anal. At. Spectrom. 19 (7) (2004) 815–822, doi:10.1039/b403128h.

[10] X. Yan, Z. Ni, [Speciation of metals and metalloids in biomolecules by hyphenated techniques], Guang Pu Xue Yu Guang Pu Fen Xi Guang Pu 21 (2) (2001) 129–138.

[11] J. Galceran, E. Companys, J. Puy, J. Cecilia, J.L. Garces, AGNES: a new electroanalytical technique for measuring free metal ion concentration, J. Electroanal. Chem. 566 (1) (2004) 95–109.

[12] J. Wang, B. Tian, J. Wang, Electrochemical flow sensor for in-situ monitoring of total metal concentrations, Anal. Commun. 35 (8) (1998) 241–243, doi:10.1039/A803525C.

[13] A.K. Malik, J.S. Aulakh, V. Kaur, Metal ions analysis with capillary zone electrophoresis, Methods Mol. Biol. Clifton NJ 1483 (2016) 217–247, doi:10.1007/978-1-4939-6403-1_13.

[14] K. Fytianos, Speciation analysis of heavy metals in natural waters: a review, J. AOAC Int. 84 (6) (2001) 1763–1769, doi:10.1093/jaoac/84.6.1763.

[15] D.L. Parkhurst and C.A.J. Appelo, 'Description of Input and Examples for PHREEQC Version 3—A Computer Program for Speciation, Batch-Reaction, One-Dimensional Transport, and Inverse Geochemical Calculations: U.S. Geological Survey Techniques and Methods, book 6, chap. pp. A43, 497, (2013). https://pubs.usgs.gov/tm/06/a43/.

[16] M.G. Keizer, Basic principles of chemical speciation calculations, Soil Pollut. Soil Prot. (1996) 137–153.

[17] B. Hribar, N.T. Southall, V. Vlachy, K.A. Dill, How ions affect the structure of water, J. Am. Chem. Soc. 124 (41) (2002) 12302–12311, doi:10.1021/ja026014h.

[18] C.F. Poole, Ionic Liquids, in: I.D. Wilson (Ed.), Encyclopedia of Separation Science, Academic Press, Oxford, 2007, pp. 1–8, doi:10.1016/B978-012226770-3/10680-6.

[19] H.F. Hemond, E.J. Fechner, Chapter 1 - basic concepts, in: H.F. Hemond, E.J. Fechner (Eds.), Chemical Fate and Transport in the Environment, Third Edition, Academic Press, Boston, 2015, pp. 1–73, doi:10.1016/B978-0-12-398256-8.00001-3.

[20] C.F. Ross, 2.02 - headspace analysis, in: J. Pawliszyn (Ed.), Comprehensive Sampling and Sample Preparation, Academic Press, Oxford, 2012, pp. 27–50, doi:10.1016/B978-0-12-381373-2.00036-3.

[21] F. Millero, Effects of pressure and temperature on activity coefficients, Act. Coeff. Electrolyte Solut. 2 (1979) 89.

[22] H.C. Helgeson, Prediction of the thermodynamic properties of electrolytes at high pressures and temperatures, Phys. Chem. Earth 13-14 (1981) 133–177, doi:10.1016/0079-1946(81)90009-4.

[23] H.C. Helgeson, D.H. Kirkham, Theoretical prediction of the thermodynamic behavior of aqueous electrolytes at high pressures and temperatures; II, Debye-Huckel parameters for activity coefficients and relative partial molal properties, Am. J. Sci. 274 (10) (1974) 1199–1261, doi:10.2475/ajs.274.10.1199.

[24] L.A. Bromley, Thermodynamic properties of strong electrolytes in aqueous solutions, AIChE J 19 (2) (1973) 313–320, doi:10.1002/aic.690190216.

[25] K.S. Pitzer (Ed.), Activity Coefficients in Electrolyte Solutions, Boca Raton, 1991, doi:10.1201/9781351069472.

[26] J.F. Zemaitis, D.M. Clark, M. Rafal, N.C. Scrivner, Activity coefficients of single strong electrolytes, in: Handbook of Aqueous Electrolyte Thermodynamics, John Wiley & Sons, Ltd, 1986, pp. 46–203, doi:10.1002/9780470938416.ch4.

[27] J.R. Black, Debye-Hückel equation, in: W.M. White (Ed.), Encyclopedia of Geochemistry: A Comprehensive Reference Source On the Chemistry of the Earth, Springer International Publishing, Cham, 2016, pp. 1–3, doi:10.1007/978-3-319-39193-9_61-1.

[28] J. Kielland, Individual activity coefficients of ions in aqueous solutions, J. Am. Chem. Soc. 59 (9) (1937) 1675–1678, doi:10.1021/ja01288a032.

[29] H.C. Helgeson, Thermodynamics of complex dissociation in aqueous solution at elevated temperatures, J. Phys. Chem. 71 (10) (1967) Art. no. 10, doi:10.1021/j100869a002.

[30] J.W. Tester, M. Modell, Thermodynamics and Its Applications, Prentice Hall PTR, Upper Saddle River, N.J., 1997.

[31] C.G. Patterson, D.D. Runnells, Geochemistry, low-temperature, in: R.A. Meyers (Ed.), Encyclopedia of Physical Science and Technology, Third Edition, Academic Press, New York, 2003, pp. 531–547, doi:10.1016/B0-12-227410-5/00281-7.

[32] D. Langmuir, Aqueous Environmental Geochemistry, Prentice Hall, Upper Saddle River, N.J., 1997.

[33] D.L. Parkhurst, Ion-association models and mean activity coefficients of various salts, in: *Chemical Modeling of Aqueous Systems II*, in ACS Symposium Series, 416, American Chemical Society, 1990, pp. 30–43, doi:10.1021/bk-1990-0416.ch003.

[34] N. Plummer, B.F. Jones, A.H. Truesdell, WATEQF; a FORTRAN IV version of WATEQ: a computer program for calculating chemical equilibrium of natural waters, Dept. of the Interior, Geological Survey, Water Resources Division (1976) USGS Numbered Series 76-13, doi:10.3133/wri7613.

[35] O. Söhnel, J. Garside, Precipitation: Basic Principles and Industrial Applications, Butterworth-Heinemann, Oxford [England]; Boston, 1992 ISBN 0750611073.

[36] L.L. Lee, Molecular Thermodynamics of Electrolyte Solutions, WORLD SCIENTIFIC, 2008, doi:10.1142/6836.

[37] K.S. Pitzer, 'Thermodynamics of electrolytes. I. Theoretical basis and general equations', ACS Publications, (2002). https://pubs.acs.org/doi/pdf/10.1021/j100621a026

[38] G.M. Anderson and D.A. Crerar, *Thermodynamics in Geochemistry: the Equilibrium Model*. (1993), ISBN 019506464X.

[39] B.C. Blakey, V.G. Papangelakis, A study of solid-aqueous equilibria by the speciation approach in the hydronium alunite-sulfuric acid-water system at high temperatures, Metall. Mater. Trans. B 27 (4) (1996) Art. no. 4, doi:10.1007/BF02915653.

[40] E.L. Shock, H.C. Helgeson, Calculation of the thermodynamic and transport properties of aqueous species at high pressures and temperatures: correlation algorithms for ionic species and equation of state predictions to 5 kb and 1000 °C, Geochim. Cosmochim. Acta 52 (8) (1988) 2009–2036, doi:10.1016/0016-7037(88)90181-0.

[41] J.H. Hoff, *Studies in Chemical Dynamics*. F. Muller, (1896).

[42] J.W. Cobble, R.C. Murray Jr., P.J. Turner, and K. Chen, 'High-temperature thermodynamic data for species in aqueous solution', (1982).

[43] G.M. Anderson, S. Castet, J. Schott, R.E. Mesmer, The density model for estimation of thermodynamic parameters of reactions at high temperatures and pressures, Geochim. Cosmochim. Acta 55 (7) (1991) Art. no. 7, doi:10.1016/0016-7037(91)90022-W.

[44] I. Puigdomenech, J. Rard, and I. Grenthe, *Temperature Corrections to Thermodynamic Data and Enthalpy Calculations*. (1999).

[45] C.-W. Wang, et al., Prediction of the ideal-gas thermodynamic properties for water, J. Mol. Liq. 321 (2021) 114912, doi:10.1016/j.molliq.2020.114912.

[46] M. Batzle, Z. Wang, Seismic properties of pore fluids, Geophysics 57 (11) (1992) 1396–1408 Nov., doi:10.1190/1.1443207.

[47] K. Tödheide, Water at high temperatures and pressures, in: F. Franks (Ed.), The Physics and Physical Chemistry of Water, Springer New York, Water. Boston, MA, 1972, pp. 463–514, doi:10.1007/978-1-4684-8334-5_13. in.

[48] K.J. Jackson, H.C. Helgeson, Chemical and thermodynamic constraints on the hydrothermal transport and deposition of tin: I. Calculation of the solubility of cassiterite at high pressures and temperatures, Geochim. Cosmochim. Acta 49 (1) (1985) 1–22.

[49] Thermoddem database, 'THERMOCHEMICAL AND MINERALOGICAL TABLES FOR GEOCHEMICAL MODELING', © 2020. https://thermoddem.brgm.fr/(accessed Jun. 29, 2022).

[50] R.E. Connick, R.E. Powell, The entropy of aqueous oxy-anions, J. Chem. Phys. 21 (12) (1953) 2206–2207, doi:10.1063/1.1698812.

[51] H.C. Helgeson, D.H. Kirkham, Theoretical prediction of the thermodynamic behavior of aqueous electrolytes at high pressures and temperatures; I, Summary of the thermodynamic/electrostatic properties of the solvent, Am. J. Sci. 274 (10) (1974) 1089–1198 a, doi:10.2475/ajs.274.10.1089.

[52] E.L. Shock, D.C. Sassani, M. Willis, D.A. Sverjensky, Inorganic species in geologic fluids: correlations among standard molal thermodynamic properties of aqueous ions and hydroxide complexes, Geochim. Cosmochim. Acta 61 (5) (1997) 907–950, doi:10.1016/S0016-7037(96)00339-0.

[53] G.K. Vemulapalli, Thermodynamics in chemistry, in: A.I. Woody, R.F. Hendry, P. Needham (Eds.), Philosophy of Chemistry, Handbook of the Philosophy of Science, Amsterdam: North-Holland, 2012, pp. 467–494, doi:10.1016/B978-0-444-51675-6.50030-X. 6.

[54] A.W. Hakin, M.M.H. Bhuiyan, Chapter 7: heat capacity of electrolyte solutions, Heat Capacit. (2010) 132–152, doi:10.1039/9781847559791-00132.

[55] L.G. Hepler, J.K. Hovey, Standard state heat capacities of aqueous electrolytes and some related undissociated species, Can. J. Chem. 74 (5) (1996) 639–649, doi:10.1139/v96-069.

[56] M.C.F. Magalhães, E. Königsberger, P.M. May, G. Hefter, Heat capacities of concentrated aqueous solutions of sodium sulfate, sodium carbonate, and sodium hydroxide at 25 °C, J. Chem. Eng. Data 47 (3) (2002) 590–598, doi:10.1021/je010314h.

[57] S.L. Clegg, J.A. Rard, K.S. Pitzer, Thermodynamic properties of 0-6 mol kg-1 aqueous sulfuric acid from 273.15 to 328.15 K, J. Chem. Soc. Faraday Trans. 90 (13) (1994) 1875–1894, doi:10.1039/FT9949001875.

[58] P.P.S. Saluja, D.J. Jobe, J.C. LeBlanc, R.J. Lemire, Apparent molar heat capacities and volumes of mixed electrolytes: [NaCl(aq) + CaCl2(aq)], [NaCl(aq) + MgCl2(aq)], and [CaCl2(aq) + MgCl2(aq)], J. Chem. Eng. Data 40 (2) (1995) 398–406, doi:10.1021/je00018a007.

[59] K. Ballerat-Busserolles, T.D. Ford, T.G. Call, E.M. Woolley, Apparent molar volumes and heat capacities of aqueous acetic acid and sodium acetate at temperatures fromT= 278.15 K toT= 393.15 K at the pressure 0.35MPa, J. Chem. Thermodyn. 31 (6) (1999) 741–762 Jun., doi:10.1006/jcht.1999.0484.

[60] J.J. Manyà, M.J. Antal, Review of the apparent molar heat capacities of NaCl(aq), HCl(aq), and NaOH(aq) and their representation using the Pitzer model at temperatures from (298.15 to 493.15) K, J. Chem. Eng. Data 54 (8) (2009) 2158–2169, doi:10.1021/je8009946.
[61] H.C. Helgeson, D.H. Kirkham, G.C. Flowers, Theoretical prediction of the thermodynamic behavior of aqueous electrolytes by high pressures and temperatures; IV, Calculation of activity coefficients, osmotic coefficients, and apparent molal and standard and relative partial molal properties to 600 °C and 5kb, Am. J. Sci. 281 (1981) 1249–1516, doi:10.2475/ajs.281.10.1249.
[62] C.M. Criss, F.J. Millero, Modeling the heat capacities of aqueous 1−1 electrolyte solutions with Pitzer's equations, J. Phys. Chem. 100 (4) (1996) 1288–1294, doi:10.1021/jp951355l.
[63] D.G. Archer, J.A. Rard, Isopiestic investigation of the osmotic and activity coefficients of aqueous MgSO4 and the solubility of MgSO4·7H2O(cr) at 298.15 K: thermodynamic properties of the MgSO4 + H2O system to 440 K, J. Chem. Eng. Data 43 (5) (1998) 791–806, doi:10.1021/je980047o.
[64] E.L. Shock, D.C. Sassani, M. Willis, D.A. Sverjensky, Inorganic species in geologic fluids: correlations among standard molal thermodynamic properties of aqueous ions and hydroxide complexes, Geochim. Cosmochim. Acta 61 (5) (1997) Art. no. 5, doi:10.1016/S0016-7037(96)00339-0.
[65] V.B. Parker, Thermal properties of aqueous uni-univalent electrolytes, NSRDS-NBS, Dept. of Commerce, National Bureau of Standards U.S. G.P.O, Washington, D.C: U.S, 1965.
[66] C.M. Criss, F.J. Millero, Modeling heat capacities of high valence-type electrolyte solutions with Pitzer's equations, J. Solut. Chem. 28 (7) (1999) 849–864, doi:10.1023/A:1021732214671.
[67] M.H. Abraham, Y. Marcus, The thermodynamics of solvation of ions. Part 1.—The heat capacity of hydration at 298.15 K, J. Chem. Soc. Faraday Trans. 1 Phys. Chem. Condens. Phases 82 (10) (1986) 3255–3274, doi:10.1039/F19868203255.
[68] R.C. Phutela, K.S. Pitzer, Heat capacity and other thermodynamic properties of aqueous magnesium sulfate to 473 K, J Phys Chem U. S. 90 (5) (1986), doi:10.1021/j100277a037.
[69] E.M. Woolley, L.G. Hepler, Heat capacities of weak electrolytes and ion association reactions: method and application to aqueous MgSO4 and HIO3 at 298 K, Can. J. Chem. 55 (1) (1977) 158–163, doi:10.1139/v77-027.
[70] C. Jolicoeur, J. Boileau, S. Bazinet, P. Picker, Thermodynamic properties of aqueous organic solutes in relation to their structure. Part II. apparent molal volumes and heat capacities of c-alkylamine hydrobromides in water, Can. J. Chem. 53 (5) (1975) 716–722, doi:10.1139/v75-100.
[71] P.A. Leduc, J.L. Fortier, J.E. Desnoyers, Apparent molal volumes, heat capacities, and excess enthalpies of n-alkylamine hydrobromides in water as a function of temperature, J. Phys. Chem. 78 (12) (1974) 1217–1225, doi:10.1021/j100605a017.
[72] G. Perron, J.-L. Fortier, J.E. Desnoyers, The apparent molar heat capacities and volumes of aqueous NaCl from 0.01 to 3 mol kg−1 in the temperature range 274.65 to 318.15 K, J. Chem. Thermodyn. 7 (12) (1975) 1177–1184, doi:10.1016/0021-9614(75)90039-7.
[73] D.J. Bradley, K.S. Pitzer, Thermodynamics of electrolytes. 12. Dielectric properties of water and Debye-Hueckel parameters to 350.degree.C and 1 kbar, J. Phys. Chem. 83 (12) (1979) 1599–1603, doi:10.1021/j100475a009.
[74] D.P. Fernández, A.R.H. Goodwin, E.W. Lemmon, J.M.H. Levelt Sengers, R.C. Williams, A formulation for the static permittivity of water and steam at temperatures from 238 K to 873 K at pressures up to 1200 MPa, including derivatives and Debye-Hückel coefficients, J. Phys. Chem. Ref. Data 26 (4) (1997) 1125–1166, doi:10.1063/1.555997.
[75] D.G. Archer, P. Wang, The dielectric constant of water and Debye-Hückel limiting law slopes, J. Phys. Chem. Ref. Data 19 (2) (1990) 371–411, doi:10.1063/1.555853.
[76] J.A. Rard, D.G. Miller, Isopiestic determination of the Osmotic coefficients of aqueous sodium sulfate, magnesium sulfate, and sodium sulfate-magnesium sulfate at 25 .degree.C, J. Chem. Eng. Data 26 (1) (1981) 33–38, doi:10.1021/je00023a013.
[77] P.P. Saluja, J.C. LeBlanc, H.B. Hume, Apparent molar heat capacities and volumes of aqueous solutions of several 1:1 electrolytes at elevated temperatures, Can. J. Chem. 64 (5) (1986) 926–931 a, doi:10.1139/v86-153.
[78] P.P. Saluja, K.S. Pitzer, R.C. Phutela, High-temperature thermodynamic properties of several 1:1 electrolytes, Can. J. Chem. 64 (7) (1986) 1278–1285, doi:10.1139/v86-220.
[79] V.G. Papangelakis, G.P. Demopoulos, Acid pressure oxidation of arsenopyrite: part i, reaction chemistry, Can. Metall. Q. 29 (1) (1990) 1–12, doi:10.1179/cmq.1990.29.1.1.
[80] D. Filippou, G.P. Demopoulos, V.G. Papangelakis, Hydrogen ion activities and species distribution in mixed metal sulfate aqueous systems, AIChE J. 41 (1) (1995) 171–184, doi:10.1002/aic.690410117.
[81] D.D. Wagman, et al., Erratum: the NBS tables of chemical thermodynamic properties. Selected values for inorganic and C1 and C2 organic substances in SI units, J. Phys. Chem. Ref. Data 18 (4) (1989) 1807–1812, doi:10.1063/1.555845.
[82] J.M. Casas, V.G. Papangelakis, H. Liu, Performance of three chemical models on the high-temperature aqueous Al2(SO4)3−MgSO4−H2SO4−H2O system, Ind. Eng. Chem. Res. 44 (9) (2005) 2931–2941, doi:10.1021/ie049535h.
[83] C.F. Baes, R.E. Mesmer, The Hydrolysis of Cations, Wiley, New York, 1976 ISBN 0471039853.
[84] 1 M. Baghalha, V.G. Papangelakis, The ion-association-interaction approach as applied to aqueous H2SO4-Al2(SO4)3-MgSO4 solutions at 250 °C, Metall. Mater. Trans. B 29 (5) (1998). Art. no. 5, doi:10.1007/s11663-998-0070-6.
[85] M.W. Jones, V. Papangelakis, J.D.T. Steyl, Chemical modelling of MgSO4 solubility in atmospheric chloride leaching of laterites, Hydrometall. 2008 Proc. 6th Int. Symp (2008) 561–569.
[86] P. Lu, G. Zhang, J. Apps, C. Zhu, Comparison of thermodynamic data files for PHREEQC, Earth-Sci. Rev. 225 (2022) 103888, doi:10.1016/j.earscirev.2021.103888.
[87] W.L. Marshall, R. Slusher, Aqueous systems at high temperature. XV. Solubility and hydrolytic instability of magnesium sulfate in sulfuric acid-water and deuterosulfuric acid-deuterium oxide solutions, 200° to 350 °C, J. Chem. Eng. Data 10 (4) (1965) 353–358, doi:10.1021/je60027a016.
[88] H. Liu, V.G. Papangelakis, M.S. Alam, G. Singh, Solubility of hematite in H2SO4 solutions at 230-270 °c, Can. Metall. Q. 42 (2) (2003) 199–207, doi:10.1179/cmq.2003.42.2.199.
[89] V. Umetsu, K. Tozawa, K. Sasaki, The hydrolysis of ferric sulphate solutions at elevated temperatures, Can. Metall. Q. 16 (1) (1977) 111–117, doi:10.1179/cmq.1977.16.1.111.
[90] M. Reid, V. Papangelakis, New data on hematite solubility in sulphuric acid solutions from 130 to 270 °c, Iron Control Technol (2006) 673–686.
[91] W. Bullough, T. Canning, M. Strawbridge, The solubility of ferrous sulphate in aqueous solutions of sulphuric acid, J. Appl. Chem. 2 (2007) 703–707, doi:10.1002/jctb.5010021207.
[92] F. Hasegawa, K. Tozawa, T. Nishimura, Solubility of ferrous sulfate in aqueous solutions at high temperatures, Shigen–Sozai 112 (12) (1996) 879–884, doi:10.2473/shigentosozai.112.879.
[93] W.L. Marshall, J.S. Gill, R. Slusher, Aqueous systems at high temperature—VI: investigations on the system NiOSO3H2O and its D2O analogue from 10−4 to 3 m SO3, 150-450 °C, J. Inorg. Nucl. Chem. 24 (7) (1962) 889–897, doi:10.1016/0022-1902(62)80110-9.
[94] M. Baghalha, 'Aqueous H2SO4-Al2(SO4)3-MgSO4 solutions at 250 °C, identification of chemistry and thermodynamics, and application to the pressure acid leaching of laterites', Thesis, (1999). Accessed: Jun. 14, 2022, https://tspace.library.utoronto.ca/handle/1807/12534
[95] A.G. Dickson, D.J. Wesolowski, D.A. Palmer, R.E. Mesmer, Dissociation constant of bisulfate ion in aqueous sodium chloride solutions to 250 degree C, J. Phys. Chem. U. S. 94 (1990) 20, doi:10.1021/j100383a042.
[96] W.L. Marshall, E.U. Franck, Ion product of water substance, 0-1000 °C, 1-10,000 bars new international formulation and its background, J. Phys. Chem. Ref. Data 10 (2) (1981) 295–304, doi:10.1063/1.555643.
[97] J. Temoltzi-Avila, G.A. Iglesias-Silva, M. Ramos-Estrada, Comparison among Pitzer model and solvation models. calculation of osmotic and activity coefficients and dilution enthalpy for single-electrolyte aqueous solutions, Ind. Eng. Chem. Res. 57 (31) (2018) 10684–10700, doi:10.1021/acs.iecr.8b00699.
[98] M.K. Ridley, D.J. Wesolowski, D.A. Palmer, R.M. Kettler, Association quotients of aluminum sulphate complexes in NaCl media from 50 to 125 °C: results of a potentiometric and solubility study, Geochim. Cosmochim. Acta 63 (1999) 459–472, doi:10.1016/S0016-7037(99)00016-2.
[99] O.V. Dickson, T. Deleau, C. Coquelet, F. Espitalier, J. Lombart, A. Tardy, The influence of activity coefficient and equilibrium constant models on the speciation of aqueous solutions of H2SO4-MgSO4-Al2(SO4)3 at 235 and 250 °C', Physicochem. Probl. Miner. Process. 59 (5) (2023), doi:10.37190/ppmp/167497.